

## **Distribution Agreement**

In presenting this thesis as a partial fulfillment of the requirements for a degree from Emory University, I hereby grant to Emory University and its agents the non-exclusive license to archive, make accessible, and display my thesis in whole or in part in all forms of media, now or hereafter now, including display on the World Wide Web. I understand that I may select some access restrictions as part of the online submission of this thesis. I retain all ownership rights to the copyright of the thesis. I also retain the right to use in future works (such as articles or books) all or part of this thesis.

Kexin Qu

April 15, 2014

Numerical Simulations of Blood Flow in Coronary Arteries Investigating Sensitivity of  
Numerical Results to Different Boundary Pressures at Outflow

by

Kexin Qu

Adviser

Alessandro Veneziani

Department of Mathematics and Computer Science

Alessandro Veneziani

Adviser

Shanshuang Yang

Committee Member

Howard Chang

Committee Member

2014

Numerical Simulations of Blood Flow in Coronary Arteries Investigating Sensitivity of  
Numerical Results to Different Boundary Pressures at Outflow

By

Kexin Qu

Alessandro Veneziani

Adviser

An abstract of  
a thesis submitted to the Faculty of Emory College of Arts and Sciences  
of Emory University in partial fulfillment  
of the requirements of the degree of  
Bachelor of Sciences with Honors

Department of Mathematics and Computer Science

2014

## Abstract

### Numerical Simulations of Blood Flow in Coronary Arteries Investigating Sensitivity of Numerical Results to Different Boundary Pressures at Outflow

By Kexin Qu

Atherosclerosis develops when cholesterol containing deposits (plaque) build up, and growth of such plaques can slowly narrow and harden the arteries throughout the body. Serious problems occur because narrowing of coronary arteries causes heart to receive less blood and leads to the heart attack. Coronary heart disease has been the leading cause of death in the developed world and nearly the leading cause in the developing world. As it has been found that atherosclerosis is strongly associated with local hemodynamic of blood flow, mathematical modeling is applied to build the relationship between pressures the velocities. As a result, predictions of atherosclerosis for a specific patient can be made based on the solutions to those mathematical equations. Blood in this study is considered being incompressible unsteady Newtonian fluid, and Navier Stokes equations are applied for modeling. Computational dynamic modeling (CFD) is applied to solve those problems numerically. However, to obtain reliable clinical results, the required accurate patient specific boundary conditions are hard to measure due to technical difficulties, especially the pressures on the outflow boundary. This study aimed to investigate how inaccurate pressures at outflow boundaries would affect the numerical results. In this study, five cases with different outflow pressures (baseline pressure was from patient specific measurements; two cases were with pressures increased by 10% and 20% from the baseline; the other two cases were with pressures decreased by 10% and 20% from the baseline) and the same inflow velocities were simulated within a complete cardiac cycle 0.833s. The coronary artery geometry, velocities and baseline pressures were acquired from a specific patient.

The results showed obvious pressure increases as the boundary pressures increased, whereas velocity distribution remained identical visually (clinically). Atherosclerosis risk indices, wall shear stress (WSS) and oscillatory shear index (OSI) were the clinically the same as well. At this point of study, it can be concluded that changes on the outflow boundary pressures clinically have no effect on the resulting velocities, wall shear stress and oscillatory shear index, and thus the prediction of atherosclerosis.

Numerical Simulations of Blood Flow in Coronary Arteries Investigating Sensitivity of  
Numerical Results to Different Boundary Pressures at Outflow

By

Kexin Qu

Alessandro Veneziani

Adviser

A thesis submitted to the Faculty of Emory College of Arts and Sciences  
of Emory University in partial fulfillment  
of the requirements of the degree of  
Bachelor of Sciences with Honors

Department of Mathematics and Computer Science

2014

## Acknowledgements

I would like to acknowledge my advisor, Professor Alessandro Veneziani, who invested many hours teaching and mentoring me throughout this year. I would like to thank Professor ShanShuang Yang, Professor Howard Chang for their comments on the work, and for being committee members for my defense. I would also like to thank Tiziano and Luca for spending time helping me with problems on this research project. I would like to thank Emory Mathematics department for making my four years' time great both in knowledge and in life. I would like to thank my parents for endless support and love.

# Contents

<b>1</b>	<b>Introduction</b>	<b>1</b>
1.1	Coronary Arteries and Atherosclerosis . . . . .	1
1.2	Computational Fluid Dynamics . . . . .	4
1.3	Ingredients of a CFD analysis . . . . .	5
1.4	Objective and Significance . . . . .	6
<b>2</b>	<b>Methods</b>	<b>8</b>
2.1	Simplified Assumptions . . . . .	8
2.2	The Governing Mathematical Model . . . . .	10
2.3	Quantitative Analyses . . . . .	12
2.4	CFD workflow . . . . .	12
2.5	Numerical Approximation . . . . .	13
2.5.1	Underlying Concepts . . . . .	13
2.5.2	Softwares . . . . .	14
<b>3</b>	<b>Results</b>	<b>15</b>
3.1	Physical Properties of Blood . . . . .	15
3.2	Numerical Results . . . . .	15
<b>4</b>	<b>Discussion</b>	<b>25</b>
<b>5</b>	<b>Conclusion</b>	<b>34</b>
<b>6</b>	<b>Bibliography</b>	<b>42</b>

# List of Figures

1	Anatomy of coronary arteries of the heart [13] . . . . .	1
2	Illustration of plaque growth and narrowing of blood vessels [1] . . . . .	2
3	A: Cross-sectional schematic diagram of a blood vessel illustrating hemodynamic shear stress, the frictional force per unit area acting on the inner vessel wall. B: Illustration of the range of shear stress magnitudes encountered in veins, arteries, and in low-shear and high-shear pathologic states [17]. . . . .	3
4	Geometry of the coronary artery, illustrating the computational domain. . .	11
5	Velocities evolution over a complete cardiac cycle . . . . .	15
6	Pressures evolution of five cases over a complete cardiac cycle: the baseline outflow pressure, pressures increased by 10% and by 20%, pressures decreased by 10% by 20%. . . . .	16
7	Evolution of pressure distributions within a complete cardiac cycle, for the case with 20% less outflow boundary pressures . . . . .	19
8	Evolution of pressure distributions within a complete cardiac cycle, for the case with 10% less outflow boundary pressures . . . . .	22
9	Evolution of pressure distributions within a complete cardiac cycle, with baseline boundary pressures . . . . .	25
10	Evolution of pressure distributions within a complete cardiac cycle, for the case with 10% more outflow boundary pressures . . . . .	28
11	Evolution of pressure distributions within a complete cardiac cycle, for the case with 20% more outflow boundary pressures . . . . .	31
12	Evolution of velocity distributions on the vessel wall and the corresponding ranges within a complete cardiac cycle for all the five cases . . . . .	34
13	Evolution of wall shear stress distributions on the vessel wall with the corresponding ranges are visually identical across all the cases at each time point within a complete cardiac cycle . . . . .	37



14	Distributions of time average WSS magnitudes are visually identical in all the cases where pressure is decreased by 20% or by 10%, pressure is patient specific (baseline), pressure is increased by 20% , increased by 10% . . . . .	38
15	Distributions of OSI magnitudes are visually identical in all the cases where pressure is decreased by 20% or by 10% , original pressure, pressure is increased by 20% , increased by 10% . . . . .	39
16	Wall shear stress of the bifurcation area remain low consistently at each time point within a complete cardiac cycle . . . . .	42
17	Wall shear stress of part of the main coronary artery remain low consistently at each time point within a complete cardiac cycle . . . . .	45

# 1 Introduction

## 1.1 Coronary Arteries and Atherosclerosis

Coronary arteries supply blood and nutrients to the heart muscle. They are located on the surface of the heart and consist of two main arteries: the right and left coronary arteries, and their two branches [13](Figure 1).

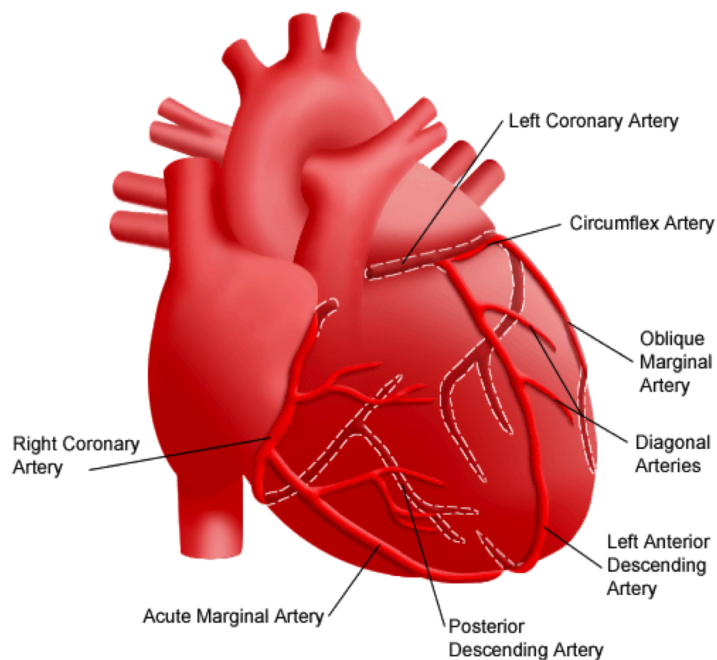


Figure 1: Anatomy of coronary arteries of the heart [13]

In the normal condition, the arteries can adapt to changes in blood flow and blood pressure (For example, as people are doing physical exercises, the heart rate will accelerate and blood pressure will increase). However, under certain circumstances, they may fail to heal themselves and can't respond to the imposed forces appropriately and in the worst case, are unable to deliver blood to the heart .

*Atherosclerosis*, develops when cholesterol containing deposits (plaque) build up, and the growth of such plaques can slowly narrow and harden the arteries throughout the body

(Figure 2). When atherosclerosis affects the arteries of the heart, it is called coronary artery

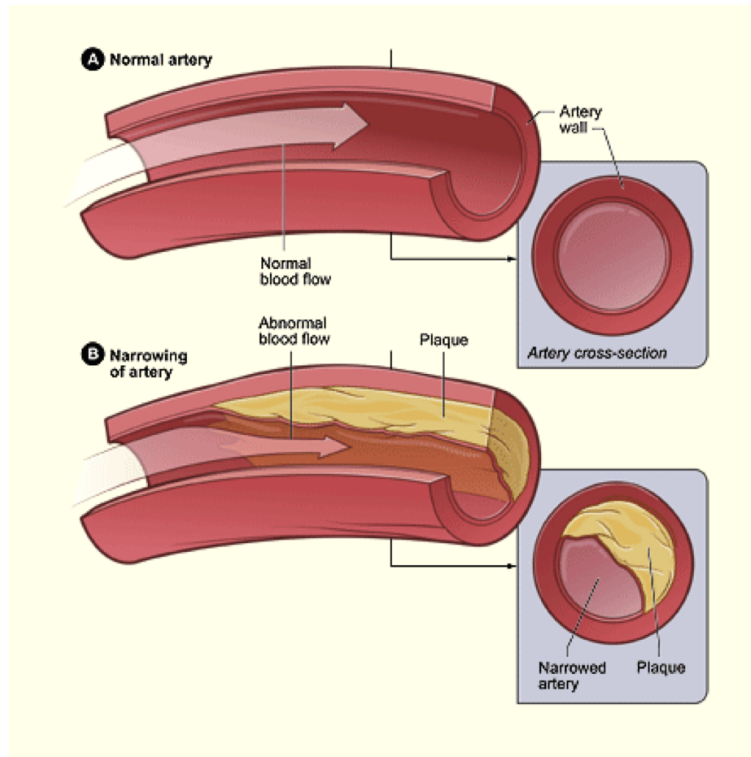


Figure 2: Illustration of plaque growth and narrowing of blood vessels [1]

disease (CAD). Narrowing of coronary arteries causes heart to receive less blood and may lead to the heart attack [1].

According to the world health organization (WHO), coronary heart disease has been the leading cause of death in the developed world and nearly the leading cause in the developing world. Although a number of risk factors including hypertension, smoking, lipid disorders and diabetes have been considered contributing to the disease, atherosclerosis remains a geometrically focal disease [18]. As atherosclerotic lesions evolve, the coronary arteries undergo local quantitative and qualitative changes in the wall, and the subsequent stiffening amplifies the local hemodynamic environment of atherosclerosis development [7]. The altered flow conditions can usually be observed in such regions, including separation and flow reversal, which are recognized by low or oscillatory shear stress [6] (Figure 3).

As a matter of fact, the disease occurs with much higher frequency at carotid bifurcation,

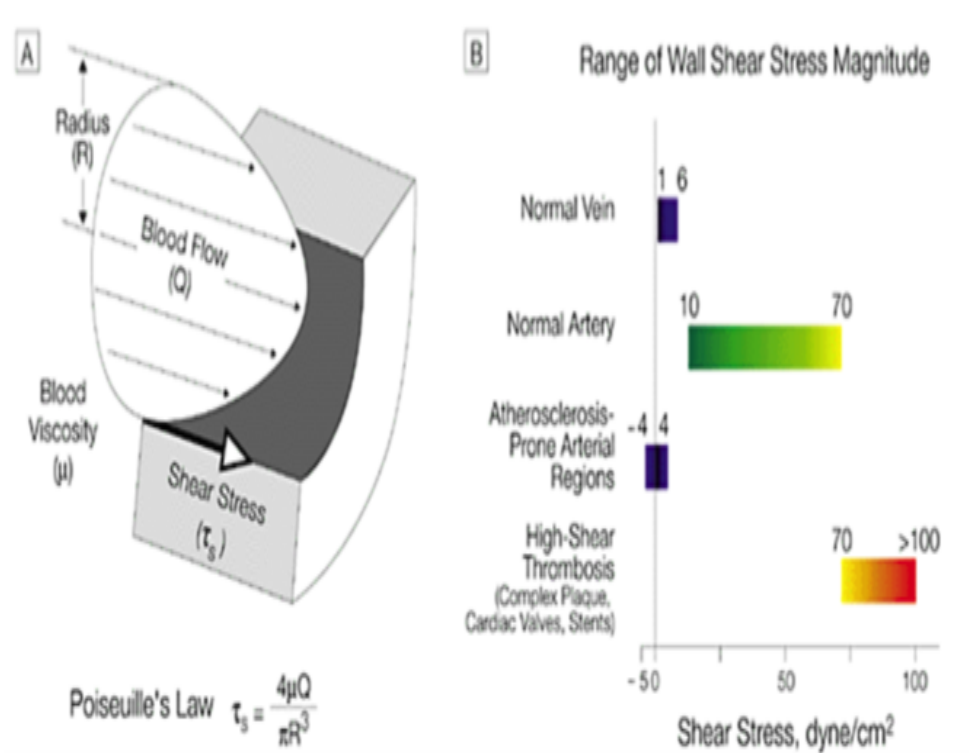


Figure 3: A: Cross-sectional schematic diagram of a blood vessel illustrating hemodynamic shear stress, the frictional force per unit area acting on the inner vessel wall. B: Illustration of the range of shear stress magnitudes encountered in veins, arteries, and in low-shear and high-shear pathologic states [17].

the coronary arteries, the abdominal aorta, and the vessels supplying the lower extremities [16]. The propensity that plaque forms at bifurcations, branching, and curvatures has been associated with local mechanical factors such as wall shear stress (WSS) and tensile stress [11]. Therefore, a detailed understanding of local hemodynamic would be beneficial to investigate the effect of vascular wall modification on flow patterns. In this context, mathematical modeling of those related parameters is introduced to help inspect the local hemodynamic and then provide predictions in terms of short and long term evolution of the disease.

## 1.2 Computational Fluid Dynamics

Computational fluid dynamics (CFD) is adopted as a tool in studying local hemodynamic of blood flow. CFD is a branch of numerical analyses dedicated to quantitative study of fluid flow problems. Fluids have various features that have made mathematical and numerical analyses still challenging. The development of systematic methods for computational analysis of fluids has made such problems solvable by using simplified assumptions. In particular, the capability of reconstructing real problems in the "virtual world" of mathematical equations makes CFD interesting for the investigation of cardiovascular diseases.

CFD has been widely adopted in solving hemodynamic problems in the past few decades [9]. The application of mathematical models, solved through efficient and accurate numerical algorithms, has made impressive progress in the interpretation of the circulatory system functionality in both physiological and pathological situations, as well as in the perspective of providing patient specific design indications to surgical planning [9]. The main reasons are the rapid advancement in the power of modern computers, progress in imaging and geometry extraction techniques as well as improvements in the mathematical modeling of the relevant physiology and pathology. The reduced time frame is expected to allow quick translations of the information from CFD into a practical procedure for the doctors to make effective decisions. Rapid development of CFD application into clinical study is motivated by the increasing incidence of atherosclerosis due to aging issue; and the consequent high health care costs calls for more efficient treatment as well.

The advantages of applying CFD practice are in the followings aspects:

1. Numerical Simulation (a.k.a, *in silico* modeling), are in general less expensive than investigations in the lab (*in vitro* or on animals (*in vivo*))
2. Numerical simulations reduce the time needed if using the traditional methods(*in vivo* and *in vitro*)to solve problems.
3. There are possibilities in studying various problems whose experiments might be difficult to conduct on real patients; or it is impossible to obtain the non-measurable parameters, such as wall shear stress and local wall pressure.
4. Being able to controlling boundary conditions. This may help the surgeons to understand different surgical situations and then provide the most appropriate surgery design for a specific patient. Numerical models of vascular flows can also provide a training platform for new surgeons.
5. Being able to help evaluate and analyze the performance of prosthetic heart valves, stents, ventricular assist devices, blood filters, etc.

### 1.3 Ingredients of a CFD analysis

In general, a numerical simulation depends on three key ingredients:

1. A mathematical model. In this study of investigating blood flow, Navier-Stokes equations are the governing equations describing all the parameters of interest, such as pressures and velocities. It should be noticed that the application of these equations required some simplified assumptions, which will be discussed in details later.
2. A three dimensional geometry model of a selected region of a blood vessel. This may be acquired through medical imaging technique, such as computed tomography (CT) angiography or magnetic resonance imaging (MRI), and then reconstructed into a 3D model using some software such as *VMTK* .

3. Boundary Data, particularly, inflow velocities and outflow pressures. Due to the complexity of vascular system, it is not possible to take the whole system under investigation; rather, we usually examine a certain part of the vessels. This gives rise to the requirements of inflow and outflow boundary conditions since the region of interest is isolated from the rest of the arterial system for a numerical simulation. These data can be retrieved through measurements (but probably effected by noise).

## 1.4 Objective and Significance

The most common boundary conditions for three-dimensional simulations of blood flow are prescribed constant pressure or traction and prescribed velocity profiles. Patient-specific boundary conditions are acquired from direct measurements of this patient and are considered the gold standard” [22]. Ideally, for accurate disease diagnoses and predictions, one would like such condition data to be obtained in such way (direct measurements). In many simulations, however, the flow distribution and pressure field in the modeled domain are unknown and hard to be prescribed at the outflow boundaries[23], either because it is difficult to measure pressures on the outflow or due to the reason that these measurements are not always part of the clinical protocols. Currently in most cases only a part of the needed data is available. A classical example of the inflow blood rate is shown below. While it is relatively easy to have the flow rate obtained by

$$Q(t) = \rho \int_{\Gamma} \mathbf{u} \bullet \mathbf{n} \quad (1)$$

where  $Q(t)$  is the time-varying flow rate,  $\mathbf{u}$  is the velocity vector,  $\mathbf{n}$  is the outward unit vector normal to  $\mathbf{u}$ .  $\rho$  is the blood density and  $\Gamma$  represents the boundary section. Mathematical model requires the prescription of  $\mathbf{u}(\mathbf{x}, t)$  in each point of  $\Gamma$ . To fill the gap, many simplifying assumptions have to be adopted. For instance, a velocity profile of  $\mathbf{g}(\mathbf{x}, t)$  is prescribed on  $\Gamma$  and scaled in such a way that the following equation can be formulated.

$$\rho \int_{\Gamma} \mathbf{g} \bullet \mathbf{v} = Q(t) \quad (2)$$

Many assumptions have to be made when imposing these boundary conditions, which include the blood flow rate, the shape of the inflow velocity profile (such as the one in the example above), distributions of flow rates in the inflow arteries, and outflow pressures, etc [19]. However, as the hemodynamic differs when not under healthy condition, and due to the fact that substantial inter-individual variability do exist in a wide range [12], some simplified assumptions may affect the quality of the numerical results.

It is worth noting that sometimes even when using patient specific boundary conditions, for an individual associated with stress, anxiety or physical exertion, and other day - to-day activities, there may be significant variations on the values of those related physical quantities (pressures or flow rates) [8]. Therefore patient-specific boundary conditions might not accurately represent the normal day-to day physiology. And therefore results might not be appropriate in predicting future behaviors of blood hemodynamic. Another aspect where potential uncertainties might reside is associated with the noises generated along when measuring blood velocities and pressures. The errors for quantitative MR angiography average measurement have been reported to be as high as 7.6% for pulsatile flow [24]. And there are 6% systematic errors and considerable random errors if measuring blood flow using ultrasound [10].

On the mathematical level, the lack of data has been largely investigated in the context of defective boundary conditions with respect to Navier-Stoke equations[21], i.e. of problems where the boundary conditions are only partially known. On the numerical computation level, prior studies have investigated how changes in the flow rates over a wide range will affect the hemodynamic variables (*WSS*, *OSI*) in the patient based model, and have shown accurate measurements of patient specific flow rates in the feeding arteries are vital to accurately reproduce those variables in the patient [22]. However, the effects of changes in outflow boundary conditions on the simulation results have not been addressed before. It is known that solutions to the governing equations of blood flow in the large arteries are highly depen-



dent on the outflow boundary conditions imposed to represent the vascular downstream of the modeled domain. Although hemodynamic factors associated with atherosclerosis, wall shear stress and oscillatory shear index, are derived from velocity, we are interested to know if the accuracy in the pressure measurement is vital in numerical simulation to accurately reproduce the velocities inside the vessel and thus the associated factors.

This study is of more importance in the clinic point of view because the measurements of outflow boundary pressures are even harder to be acquired than the inflow velocities. If it can be shown that pressure measurements need not to be accurate, a lot of labor and expenses could be reduced and the application of CFD into a clinical procedure might be widely spread. In this study, we focused on the sensitivity of numerical simulations to the variations of blood pressures at outflow. Specifically, we tried to qualitatively describe how these variations would affect the hemodynamic parameters (  $WSS$ ,  $OSI$ , time average  $WSS$ ). The baseline blood pressures were obtained from patient specific measurement .

## 2 Methods

### 2.1 Simplified Assumptions

Before introducing the governing mathematical equations, a few assumptions must be stated.

#### **Blood flow rheology**

*Rheology* describes the link between the stress to deformation and the rate of deformation during blood flow[5]. As blood is a complex suspension in an aqueous polymer solution called *plasma* and consists of red cells, white cells, and platelets [5], it's very complicated to define its rheology. In order to give an appropriate mathematical description in terms of the relationships between some parameter such as stress and strain rate tensors, the fundamental equations, *Navier-Stokes*, are formulated. This model requires the identification of blood behavior as "Newtonian". In the specific case of blood, the most prominent rheological features [14] are:

- Shear thinning behavior
- Nonlinear viscoelastic nature
- Microcirculation effects

Despite all these features above, in fact they are essentially due to the presence of red cells. Plasma itself can be considered as a Newtonian fluid, and white cells and platelets are only a small fraction of blood cells; when red cells concentrations is less than 12 % by weight, its contribution to non-Newton fluid can be negligible as well [15]. So in the framework of large and medium vessels, it is acceptable that at the first level of approximation blood rheology can be considered as a Newtonian model. This assumption gives the blood a constant viscosity and simplifies the model greatly.

### **Turbulence in blood flow**

Fluid is called *turbulent* whenever it undergoes strongly irregular fluctuations, in which velocity and pressure both changes in time and space[21]. The presence of turbulence in fluid dynamics will involve more numerical computations and sometimes demand special devices to deal with [21]. Given the experimental data from previous studies, the *disturbed flow* is absent in most parts of human vascular system, except in the ascending aorta and in the pulmonary artery [21]. And moreover, the pulsatile nature of blood circulation doesn't allow for a fully evolved turbulent phenomenon[21]. Therefore, there is no need to take turbulence into consideration.

### **Fluid Structure Interaction (FSI)**

Despite it is evident that arterial walls deform due to the action of blood, in many biomedical engineering studies this is not considered. In fact, (1) numerical solutions of FSI are highly demanding. (2) Mathematical models and related parameters for the elastic walls are somehow questionable. Therefore, for the purpose of the present work, we consider the wall as rigid.

In summary, the underlying model for the Navier-Stoke equations is the unsteady incompressible Newtonian fluid in large vessels.

## 2.2 The Governing Mathematical Model

The mathematical model for investigating incompressible Newtonian fluid inside large and medium size vessels is the famous fundamental Navier-Stoke equations,

$$\rho \frac{\partial \mathbf{u}}{\partial t} + \rho (\mathbf{u} \bullet \nabla) \mathbf{u} + \nabla p - 2\mu \nabla \bullet D(\mathbf{u}) = f \quad (3)$$

$$\nabla \bullet \mathbf{u} = 0 \quad (4)$$

The spatial domain  $\Omega \subset R^3$  is defined as the interior area of blood vessels under investigation. Here  $\rho$  denotes the fluid density,  $p$  the fluid pressure,  $\mu$  the viscosity and  $\mathbf{u}$  the velocity.  $f$  represents the exterior forces exerted on the fluid, such as gravity. The first equation comes from the conservation of linear momentum, and consists of three scalar differential equations, representing each component of the velocity. The second equation is the *incompressibility constraint* forcing the mass conservation. As the blood is assumed to the Newtonian fluid, the viscosity  $\mu$  is kept constant at 0.035 poise.  $f$  is usually set to 0 in hemodynamic. And  $\rho$  is a constant of 1.06 g/ml in this model.  $D(\mathbf{u})$  represents the velocity deformation tensor

$$D(\mathbf{u}) = \frac{\nabla \mathbf{u} + \nabla \mathbf{u}^T}{2} \quad (5)$$

Therefore,  $\mathbf{u}$  and  $P$  are left as unknowns and need to be computed.

In order for the problems to be well posed, equations(1) must be provided with appropriate conditions and prescribing the behavior of the solution at the initial time  $t_0$  and on the boundary of  $\Omega$ . let  $\Gamma$  denotes the boundary of  $\Omega$ , and it is composed of three disjoint parts. First is the vascular wall,  $\Gamma_1$ . The most natural choice will be a *non slip condition*, which prescribes the speed of the blood on the walls being the same as of the vessel. So the Dirichlet condition is assigned:

$$u(t, x) = 0 \quad x \in \Gamma_1 \quad (6)$$

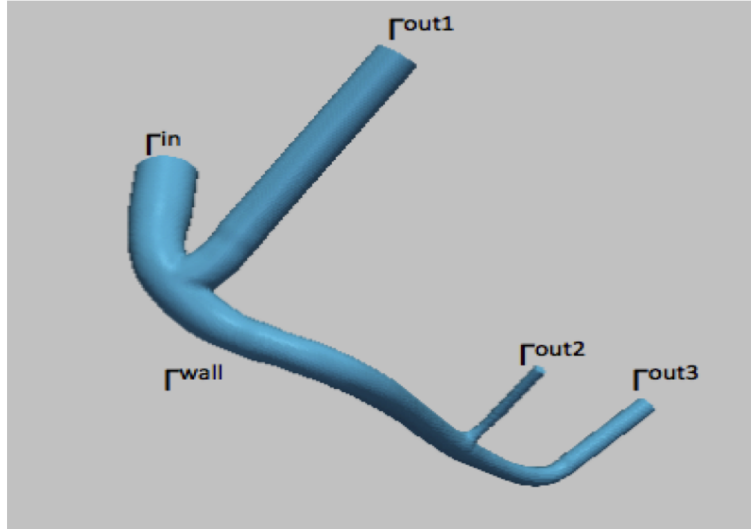


Figure 4: Geometry of the coronary artery, illustrating the computational domain.

The other two are upstream and downstream boundary conditions, corresponding respectively to the one inflow and three outflows of patient vessels (Figure 4).

It should be noticed that these are *artificial boundaries*, meaning that they are not physical interfaces but are merely used to separate the areas of interest for computational purposes. On the upstream (inflow) section, a Dirichlet condition is prescribed and the velocity from measurement of blood velocity vectors at the proximal sections are assigned. This selection is based on the simplified geometry model where the parts before upstream sections are infinitely long cylindrical pipes.

A Neumann condition is prescribed on the downstream (outflow) sections, where the *normal stresses* at the outflows are zero. Normal stress is defined as  $T \bullet \mathbf{n}$ , where  $\mathbf{n}$  is the normal vector to the boundary and  $T$  is called the *Cauchy stress tensor*:

$$T = -pI + 2\mu D(\mathbf{u}) \quad (7)$$

$I$  denotes the identity matrix. The other parameters are the same as defined in equation (3).

## 2.3 Quantitative Analyses

Three parameters were computed to indicate the responses to the variations of blood pressure on the boundary. These parameters are associated with atherosclerotic pathology and could be applied in clinic for predication.

Wall Shear Stress(wss),  $\tau_w$ , is the component of the normal stresses tangential to the wall, and is defined as the force per unit area that the fluid exerts tangentially on the wall of vessels.

$$\tau_w = \mu \frac{\partial \mathbf{u}}{\partial y}_{y=0} \quad (8)$$

where  $\mu$  is blood viscosity,  $\mathbf{u}$  is blood velocity,  $y$  is the distance to the blood wall. Wall shear stress is associated with blood velocity, and the change on it will induce the remodeling of blood endothelia and intimal thickening [18]. As plaques tend to formulate in the areas with low and oscillating WSS, it has been proposed as localizing factor of development of atherosclerosis [18]. In the susceptible areas, blood flow is slow and rapid direction changes can be observed; those altered flow patterns would result in a weak net hemodynamic shear stress. In contrast, vessel regions exposed to steady blood flow and a higher magnitude of shear stress remain comparatively disease-free [18]. Average time WSS is also computed to describe the overall behavior of wall shear stress in a complete cardiac cycle. Oscillatory Shear Index (OSI), being a WSS descriptor, is introduced to provide a numerical parameter for overall shear stress imposed on the arterial wall in a complete cardiac cycle. It is very useful in identifying regions on the vessel wall that are subjected to highly oscillating WSS directions during the cardiac cycle. Low OSI values occur where flow disruption is minimal and high OSI values usually highlights the sites where the instantaneous WSS changes rapidly in direction, such as recirculation [16].

## 2.4 CFD workflow

A brief procedure of CFD applied in this study involves the followings:

1. pre-processing:

- Obtain the medical image of the desired area of coronary artery through CT. Retrieve velocities and boundary pressures from the images, through software *Volcano*.
  - Reconstruct the 3D segments by segmenting and stacking 2D images using software *VMTK*.
  - Through *Netgen* software, reconstruct the 3-D patient model of meshes, with respect to the surface of the interested area where the flow simulations take place. The flow domain is discretized into a definite number of 3D elements (tetrahedral); numerical computation is implemented in each element.
  - Prescribe initial and boundary conditions, with data obtained in the first step.
2. Computation: perform simulations by solving appropriate mathematical equations (Navier-Stoke) through *lifeV*. Five simulations were performed, with different outflow pressures (baseline pressure was obtained from patient specific measurements; two cases were with outflow pressures increased by 10% and 20% from the baseline; the other two cases were with outflow pressures decreased by 10% and 20% from the baseline). Inflow velocities were kept the same across all the cases.
  3. Postprocessing: Use postprocessing techniques to obtain interested parameters (WSS, OSI, time average WSS). Then visualize the results through *Paraview*.

## 2.5 Numerical Approximation

### 2.5.1 Underlying Concepts

Since Navier-Stoke equations in three dimensions are too complex to be solved analytically, numerical schemes that can be implemented by computer must be introduced for approximation in both time and space.

The domain of interest was decomposed into a finite number of tetrahedrals through mesh generator *Netgen*. The software for solving problems in this study, *LifeV*, employs

Galerkin Finite Element Method for space discretization. Time is discretized into time steps of 0.0008333s. To see a detailed illustration of the method applied, one can refer to [20].

### 2.5.2 Softwares

Several softwares for simulation implementation are briefly introduced in the order by the time when they were involved.

- Scientific computing software *LifeV* [2] is used in simulation. *LifeV* is a finite element (FE) library for numerical solution of partial differential equations. The library includes solvers for incompressible fluid dynamics, linear structural problems, transport in porous media, fluid-structure interaction, etc. It is developed both for the research on new numerical algorithms as well as for providing an effective tool in solving complex "real-life" engineering problems. The case discussed in this thesis is one example of its application in cardiovascular field.
- *Netgen* [3] is an open source 2D triangular or 3D tetrahedral mesh generator. The input for 2D is described by spline curves, and the input for 3D problems can be defined by Constructive Solid Geometry (CSG), the standard STL file format, or via Boundary Representations (BRep/IGES/STEP) when compiled with OpenCascade support. NETGEN provides modules for automated mesh optimization and hierarchical mesh refinement.
- *ParaView* [4] is an open source multi-platform application based on VTK to visualize data sets of varying sizes from small to large. It provides a powerful graphical interface and offers several filters to operate on the data from numerical simulation. *ParaView* can run on distributed and shared memory parallel as well as single processor systems.

## 3 Results

### 3.1 Physical Properties of Blood

The density of blood in the simulation were set to be  $\rho = 1.06 \text{ g/cm}^3$  and viscosity were  $\mu = 0.035$  poise. The time of a whole cardiac cycle was 0.8333s.

The average velocities and pressures were derived from the medical images through the software *volcano*. Evolution of velocities within a complete cardiac cycle is shown in the plot ( Figure 5). Pressure evolution within a complete cardiac cycle, along with the four variations is described in Figure 6.

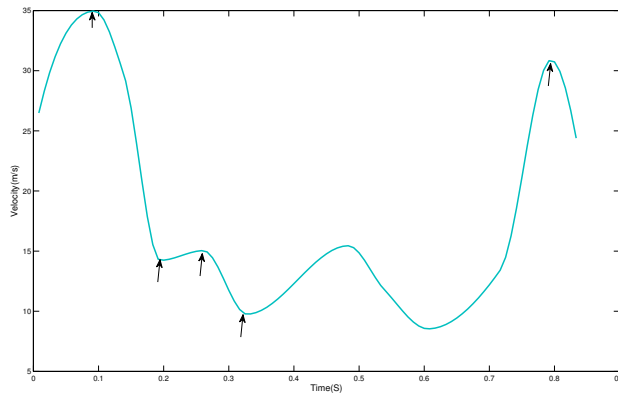


Figure 5: Velocities evolution over a complete cardiac cycle

### 3.2 Numerical Results

The mesh generated by Netgen contained 175625 elements. ( We intended to generate a finer mesh with more elements using *Netgen* . However, several attempts have resulted in failures because it involved much more computations . Due to the fact that the simulation was implemented in a student computer lab where a number of students would be using every day, too complex computations might not be feasible. Therefore, 175625 was a comprise after several failures. Since in this study the objective is mainly to qualitatively describe the sensitivity, this mesh is still good to use. ) The simulation was implemented in 0.000833s



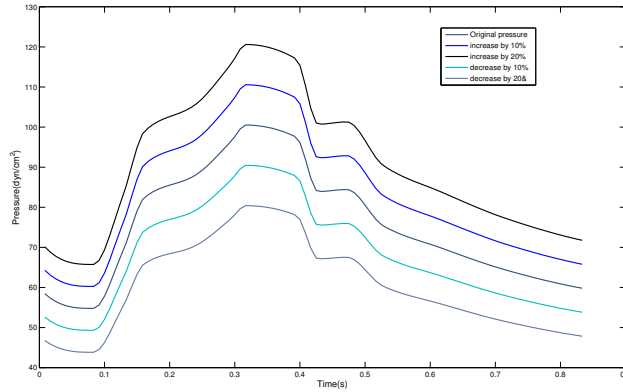


Figure 6: Pressures evolution of five cases over a complete cardiac cycle: the baseline outflow pressure, pressures increased by 10% and by 20%, pressures decreased by 10% by 20%.

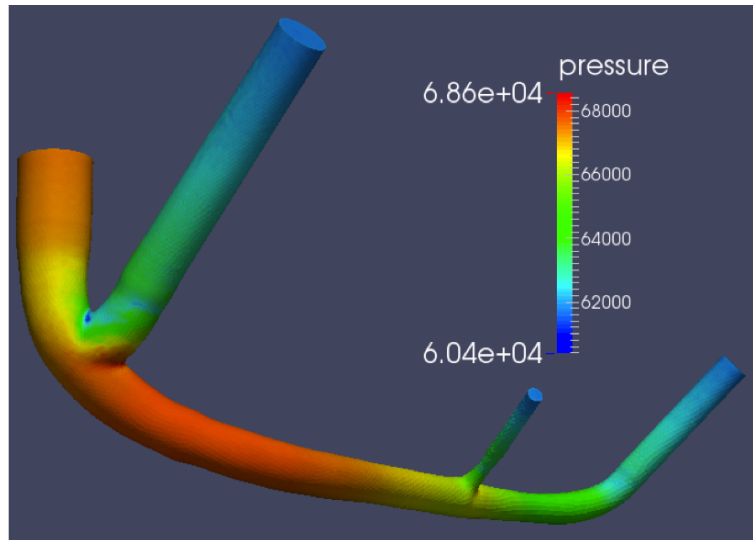
time step, saved in every 10 steps and was launched using four parallel processors.

## Pressure

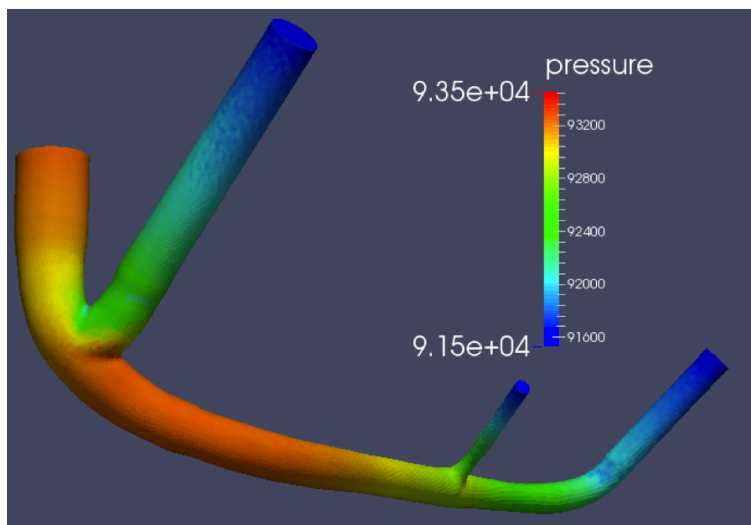
Overall, pressures increase as the outflow boundary pressures increase along the time (Figure 7-11). For illustration, five time points (0.09163s, 0.19992s, 0.25823s, 0.3332s, 0.79135s) are selected because the velocities corresponding to these moments are either local maximums or local minimums (see the arrows in Fig.5). Therefore the transition of pressures at these five points may reflect the basic nature of pressure evolution over a cardiac cycle. At each time point, the pressure range is narrow; the distributions are similar across all the cases: the highest values appear at the inflow branch and at the end of the other three branches (the outlets) comprises of low pressure magnitudes.

## Velocity

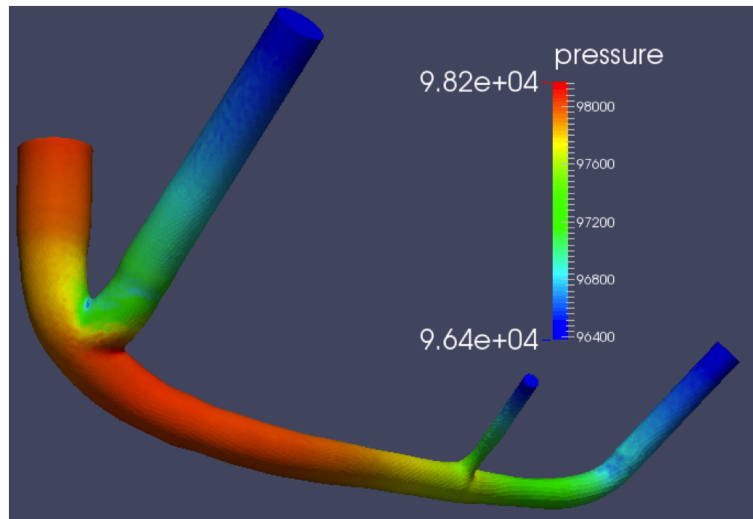
Through *paraview*, no apparent different velocities patterns are observed and ranges of magnitudes are clinically the same across all the cases at each time point (Figure 12). The values on the wall are kept zero, due to the assumption made previously. Though by direct inspection (i.e, not through *paraview* ) of the velocity values inside the vessel, some are indeed different in the ones, tens digits or digits after decimal places , the scale is too small to be



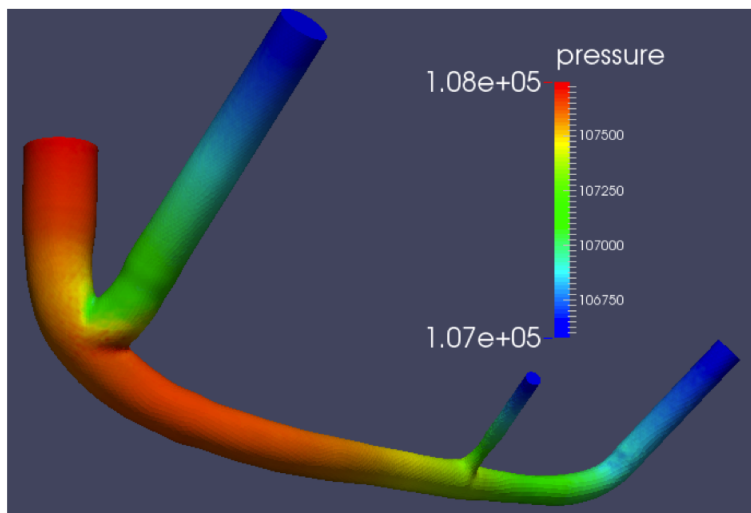
(a) pressure distribution at time 0.09163s



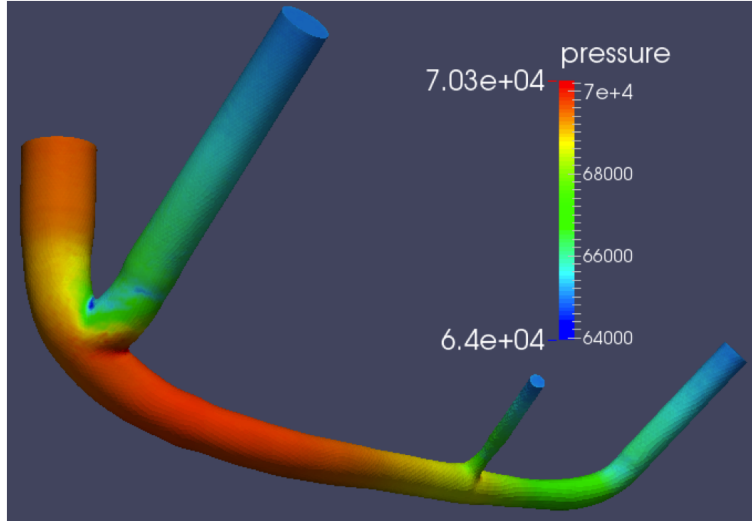
(b) pressure distribution at time 0.19992s



(c) pressure distribution at time 0.25823s



(d) pressure distribution at time 0.3332s



(e) pressure distribution at time 0.79135s

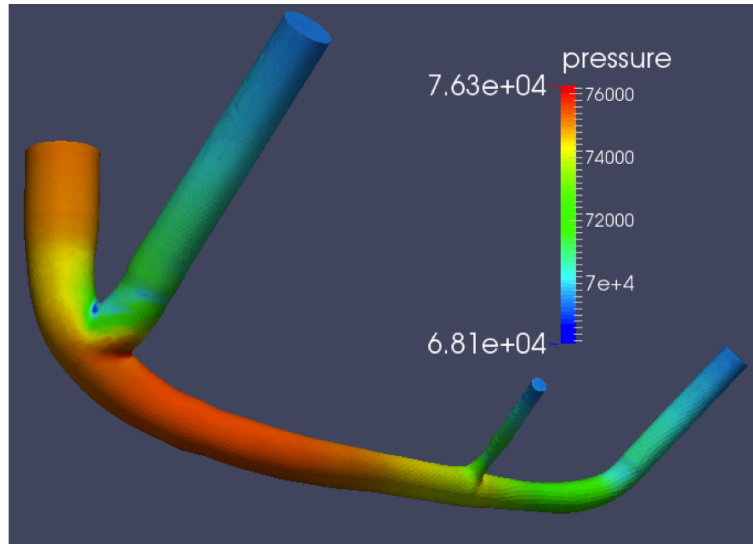
Figure 7: Evolution of pressure distributions within a complete cardiac cycle, for the case with 20% less outflow boundary pressures

considered significant in the clinical point of view.

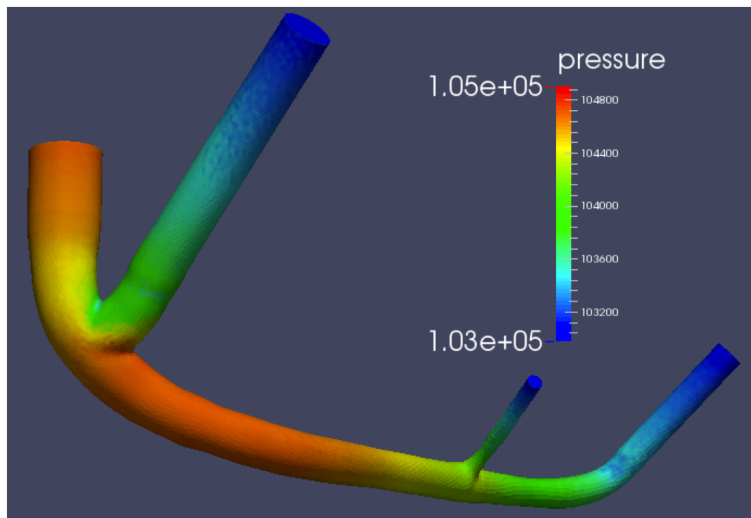
### Wall Shear Stress

Through *paraview*, no apparent different wall shear stress patterns are observed across all the cases at each time point. The ranges of magnitudes are identical as well. Though some of the values were indeed different in the ones, tens digits or digits after decimal places (by direct inspection), the scale is too small to be considered significant in the clinical point of view.

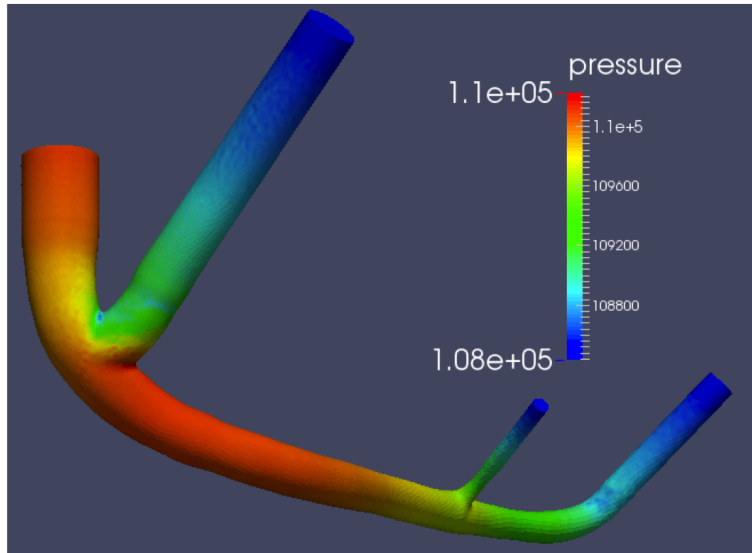
The transient distribution of the resulting wall shear stress on the blood wall over a cardiac cycle is shown in Figure 13. These five time points (0.09163s, 0.19992s, 0.25823s, 0.3332s, 0.79135s) are selected for demonstration because the velocities corresponding to these moments are either local maximums or local minimums (see the arrows in Fig. 5). Therefore the transition of wall shear stresses at these five points may reflect the basic nature of evolution over a cardiac cycle. WSS distribution resembles a similar pattern with each other across all the time points but with different shear stress ranges. WSS magnitudes



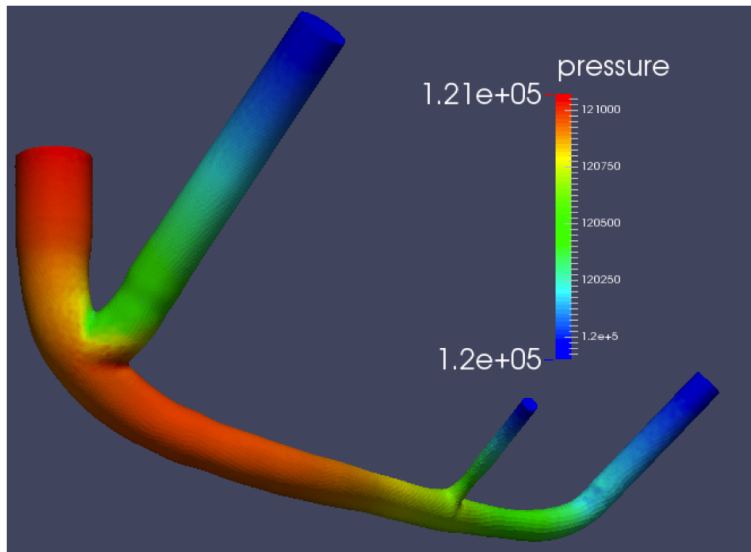
(a) pressure distribution at time 0.09163s



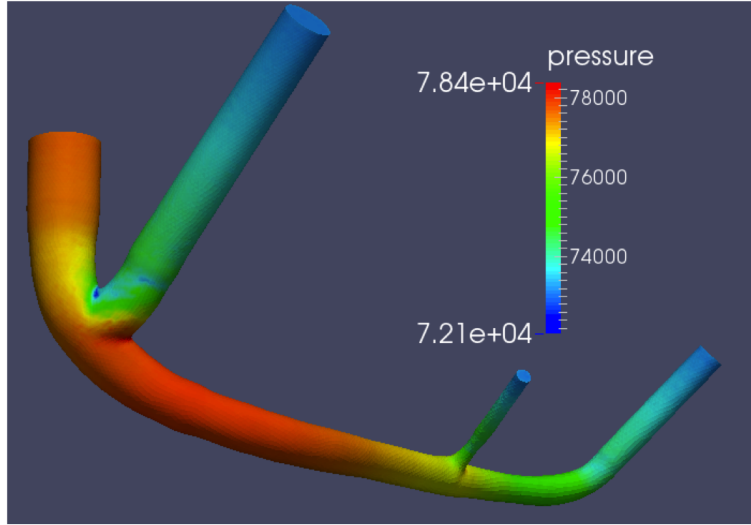
(b) pressure distribution at time 0.19992s



(c) pressure distribution at time 0.25823s



(d) pressure distribution at time 0.3332s



(e) pressure distribution at time 0.79135s

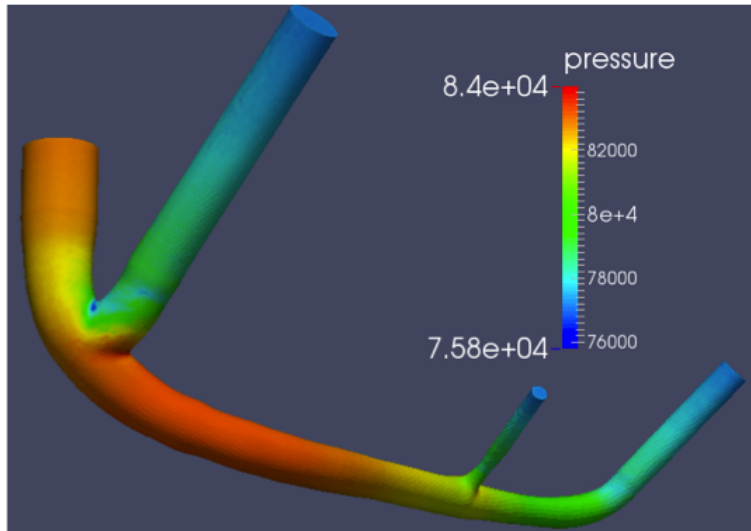
Figure 8: Evolution of pressure distributions within a complete cardiac cycle, for the case with 10% less outflow boundary pressures

remain low on the main artery (not the three branches) as time propagates. The three branches carry most of the information and could observe the highest WSS magnitudes, 265, 105, 87.7, 57.1, 211, respectively.

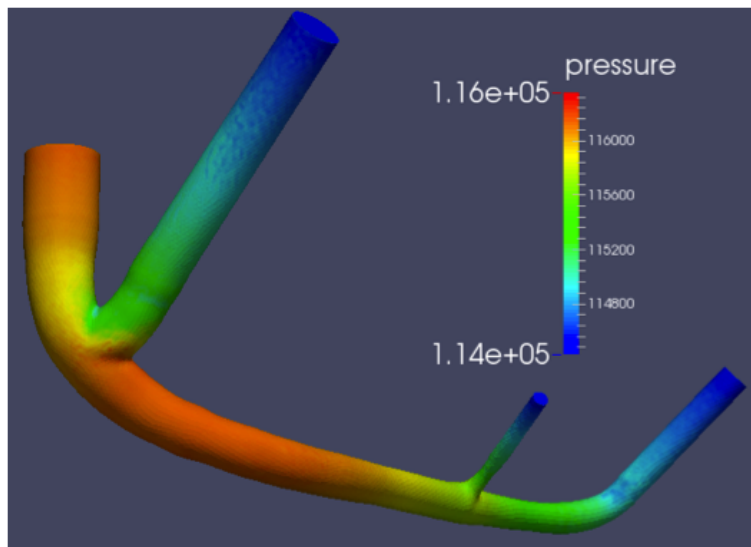
Time-average wall shear stress is also computed in order to reflect the overall behavior of wall shear stress in a complete cardiac cycle. Across all the cases, no significant difference is observed on the distribution of time average wall stress (Figure 14). Magnitude ranges are the same as well (0 to 111).

## OSI

No significant difference is observed on the distribution of oscillatory shear index (Figure 15). The ranges of values are the same as well (0 - 0.45). Although they were not completely the same by direct inspection, the scales are too tiny to be considered in the clinical point of view. Most regions on the wall have 0 OSI values, whereas on two areas the full range of OSI could be observed.

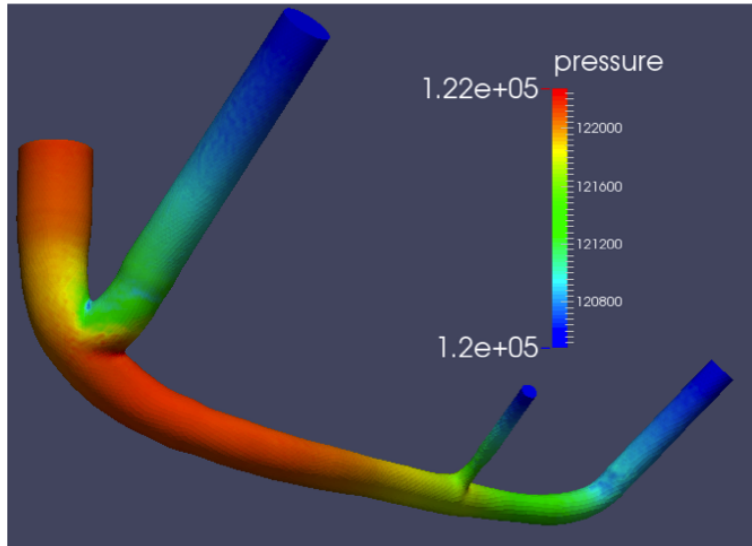


(a) pressure distribution at time 0.09163s

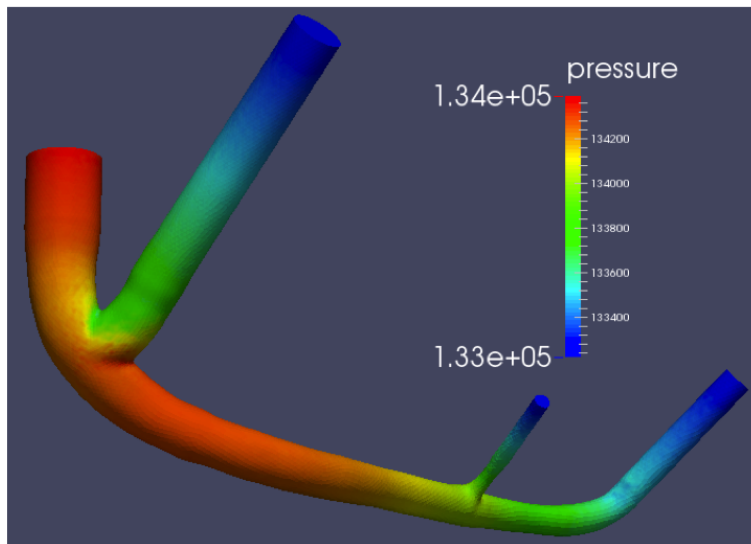


(b) pressure distribution at time 0.19992s

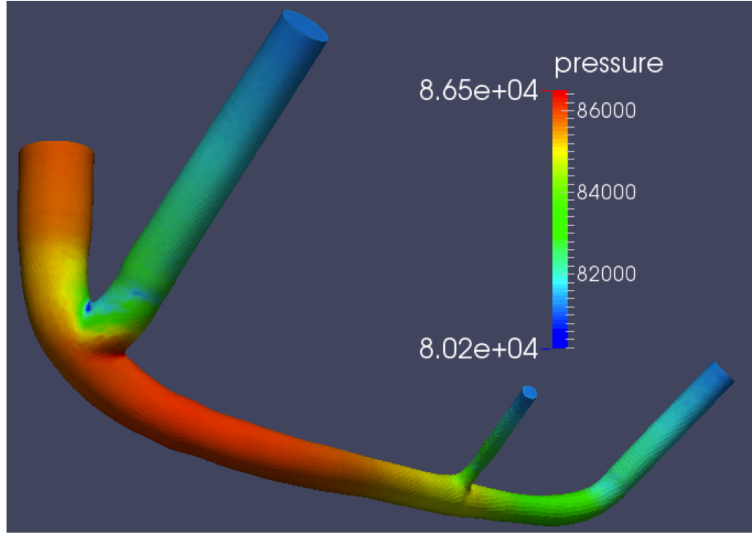




(c) pressure distribution at time 0.25823s



(d) pressure distribution at time 0.3332s



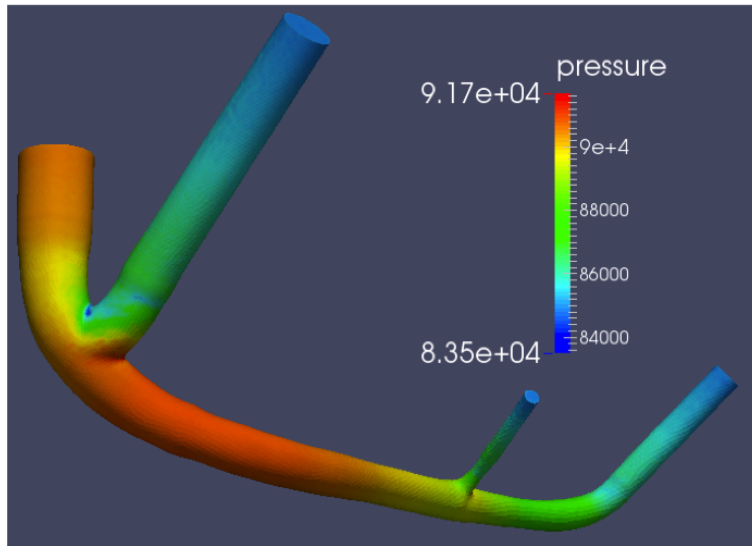
(e) pressure distribution at time 0.79135s

Figure 9: Evolution of pressure distributions within a complete cardiac cycle, with baseline boundary pressures

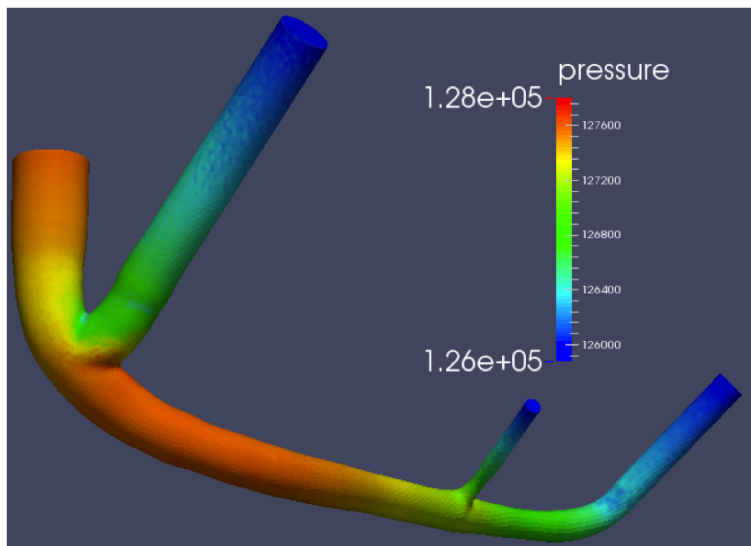
## 4 Discussion

Computational fluid dynamic (CFD) has been widely adopted in investigating blood flow problems as well as predicting pathologies in cardiovascular system. However, some simplified assumptions have to be made when building a computational model, which might generate a risk of affecting the numerical results adversely. The application of boundary conditions is one of the most important aspects. It has been known that patient-specific boundary condition is a better choice over non-patient specific data. However, due to limitations in measuring devices or being lack of time, such accurate data might not be available all the time. In this study, we are interested to investigate if little deviations from the correct data would generate any significant problems in the results, as to give wrong predications on the pathology.

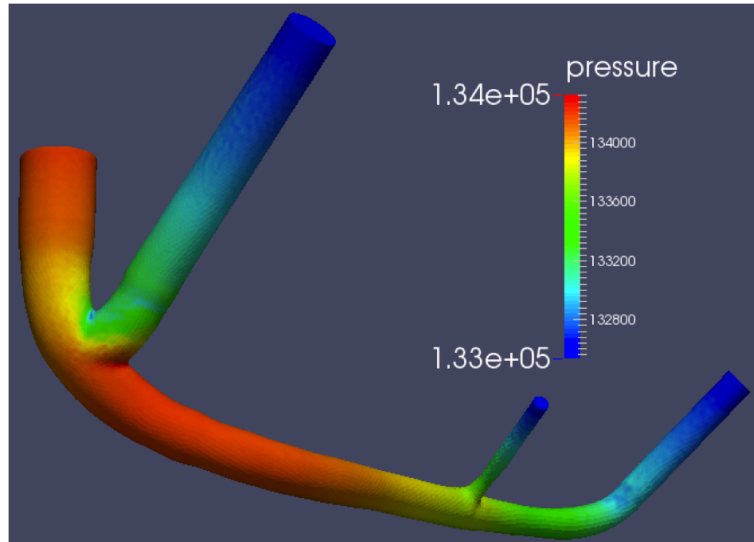
Variations of pressures on the boundaries are reflected in the resulting blood pressures. However velocities remain the same across all the cases at each time point. As being parameters derived from velocities, wall shear stress (WSS), time average wall shear stress (TAWSS),



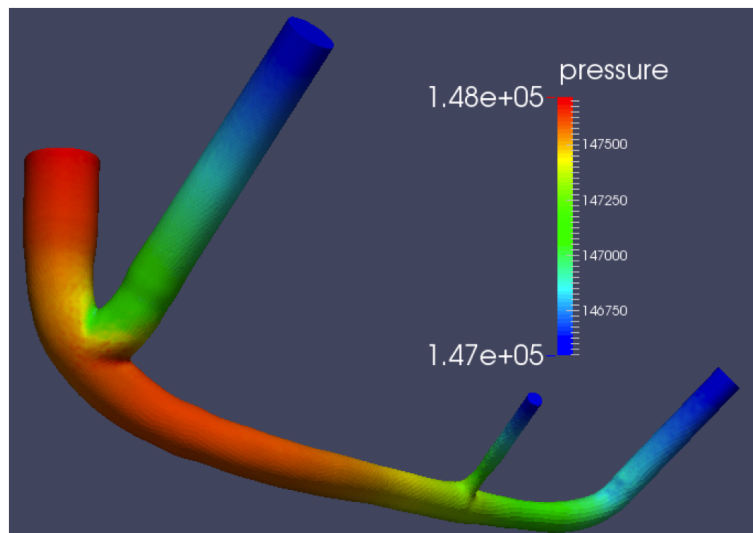
(a) pressure distribution at time 0.09163s



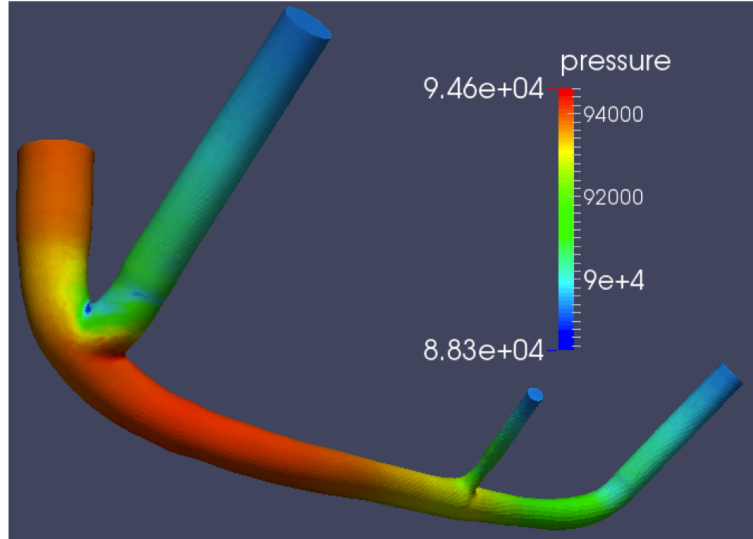
(b) pressure distribution at time 0.19992s



(c) pressure distribution at time 0.25823s



(d) pressure distribution at time 0.3332s

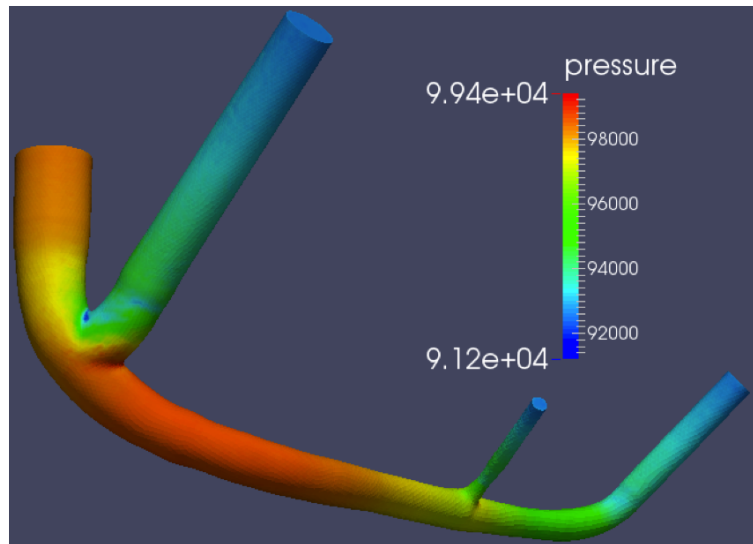


(e) pressure distribution at time 0.79135s

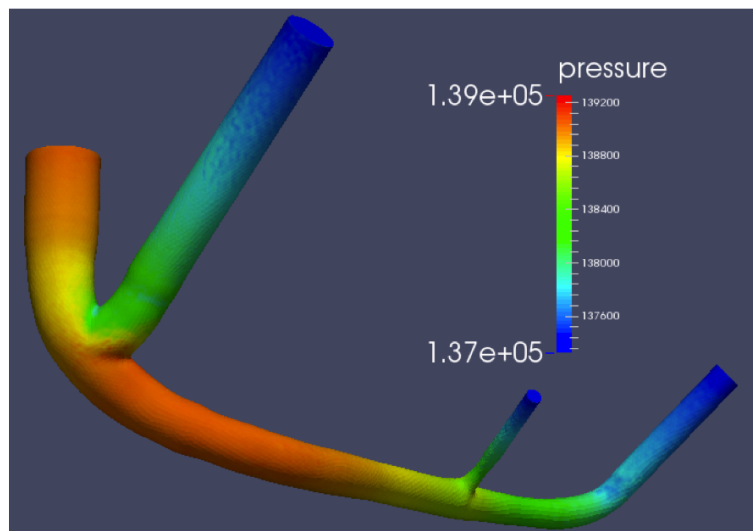
Figure 10: Evolution of pressure distributions within a complete cardiac cycle, for the case with 10% more outflow boundary pressures

and oscillatory shear index (OSI) are clinically identical as well. These results are in such consistency that they may indicate the variations (within a 20% scale from the baseline) in the boundary pressures will not affect the results of velocity and thus the parameters derived from it (WSS, OSI).

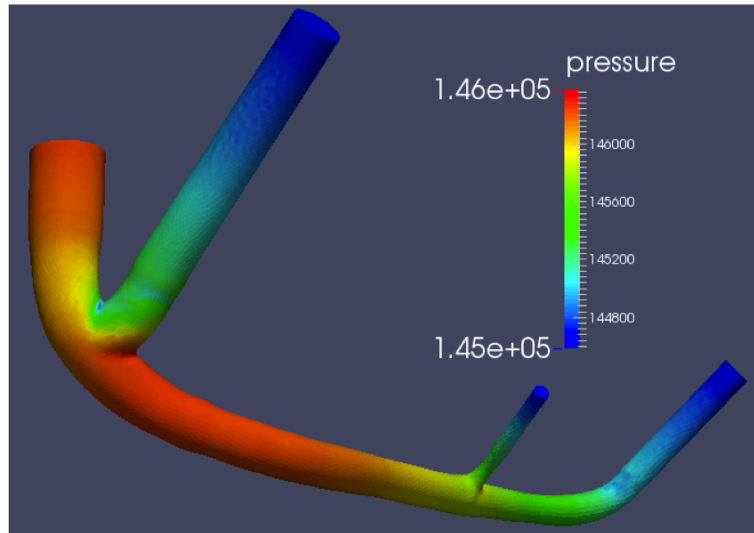
This conclusion is very favorable in clinical point of view. Due to the difficulty in measuring pressures on the downstream section of a blood vessel, if it could be shown that accuracy in boundary pressures are not important to numerically reproduce the atherosclerosis index, in the future doctors will not bother taking effort in pressure measurements. However, before drawing such a definite conclusion, some concerns and limitations need to be pointed out. As mentioned previously, due to the time constraint and feasibility of computers, the mesh adopted in this study is a compromise over a finer one, which have resulted in several failures. Therefore, there is a possibility that the results of velocities and other parameters deviate from the true values, due to the fact that the coarse mesh could generate errors that possibly have exceeded the differences between each two cases (say, between the case with baseline pressure and the case with pressures increased by 20%, etc.). When the geometry



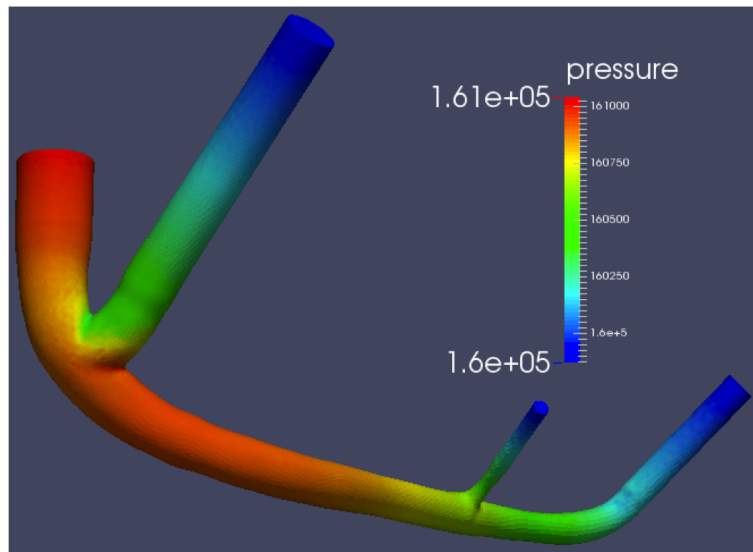
(a) pressure distribution at time 0.09163s



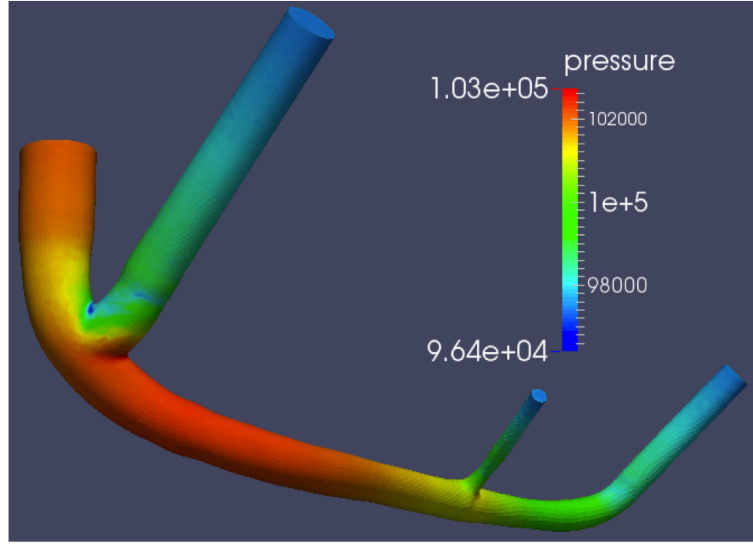
(b) pressure distribution at time 0.19992s



(c) pressure distribution at time 0.25823s



(d) pressure distribution at time 0.3332s



(e) pressure distribution at time 0.79135s

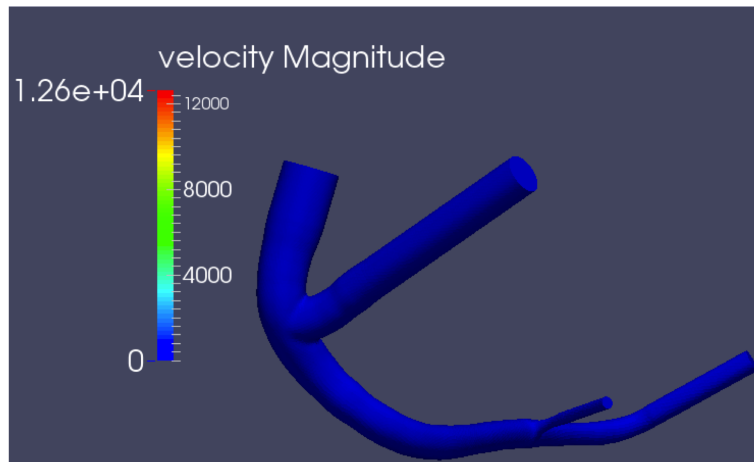
Figure 11: Evolution of pressure distributions within a complete cardiac cycle, for the case with 20% more outflow boundary pressures

is discretized into more elements that will be involved in computations, more accurate can be obtained that are closer to true values. Further studies can focus on this aspect using a finer mesh to inspect if the same conclusion could be drawn.

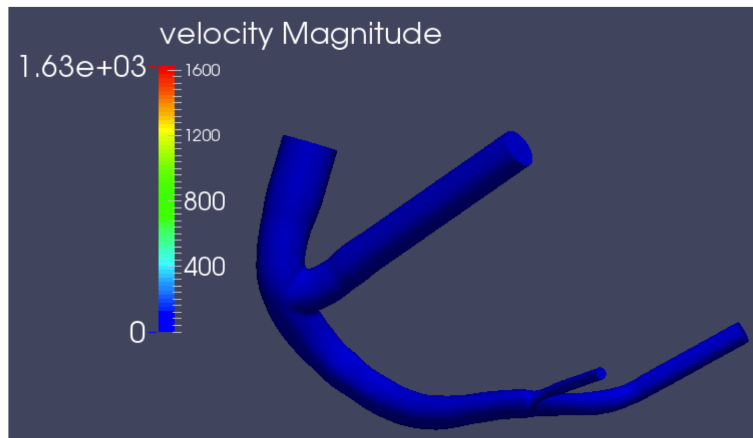
Another possibility is associated with how the pressures are varied. The pressures at three outflows are increased or decreased at the same time with a same amount. We doubt if numerically same amount of changes would counteract each other and result in the same results across all the cases. In further studies, different amount of variations on pressures could be introduced to three outflow sections respectively, and to inspect if the numerical simulation is sensitive to this kind of variation.

Based on the wall shear stress distributions (Figure 13), though values at each point change as time propagates, there are two areas where shear stress magnitudes are kept consistently low. These two areas, one in the bifurcation region (Figure 16) and one on the main coronary artery close to the bifurcation (Figure 17), are extracted for scrutinization. It could be noticed that magnitudes are mostly below 5 and a clear boundary can be observed between the dark blue regions and outer green and light blue regions. These two areas

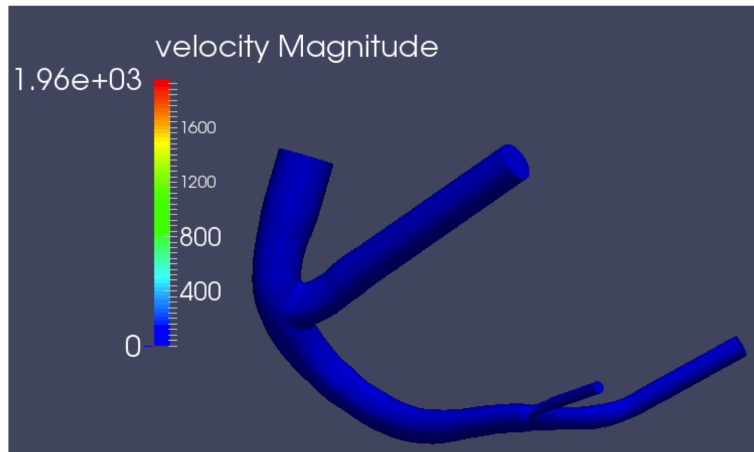




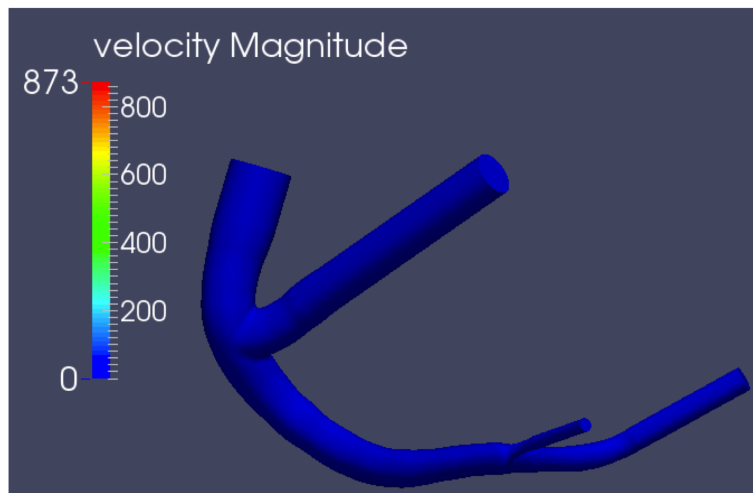
(a) Velocity distribution at time 0.09163s



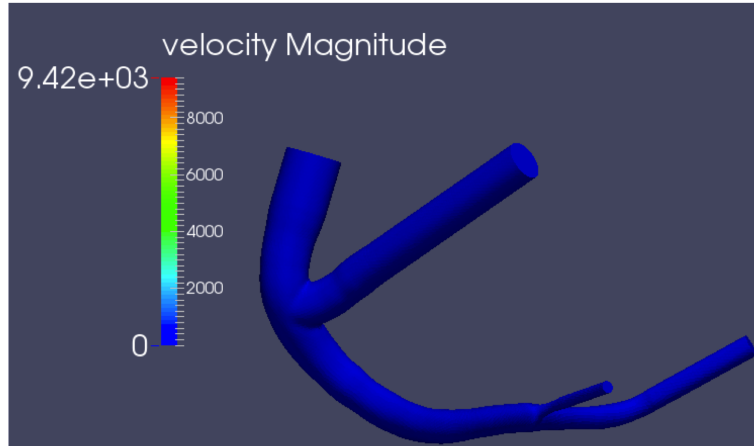
(b) Velocity distribution at time 0.19992s



(c) Velocity distribution at time 0.25823s



(d) Velocity distribution at time 0.3332s



(e) Velocity distribution at time 0.79135s

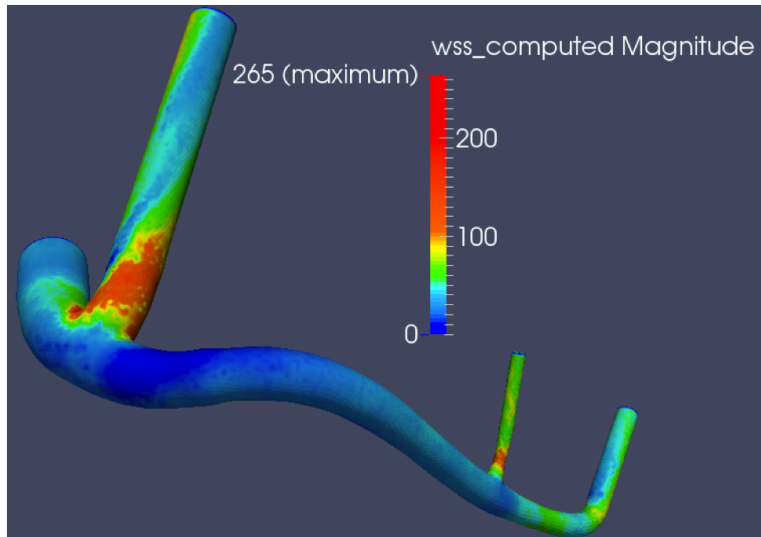
Figure 12: Evolution of velocity distributions on the vessel wall and the corresponding ranges within a complete cardiac cycle for all the five cases

correspond exactly to those two areas with high values of oscillatory shear index. This consistency confirms the association between low WSS and high OSI. Clinically, these are susceptible areas where plaques may develop.

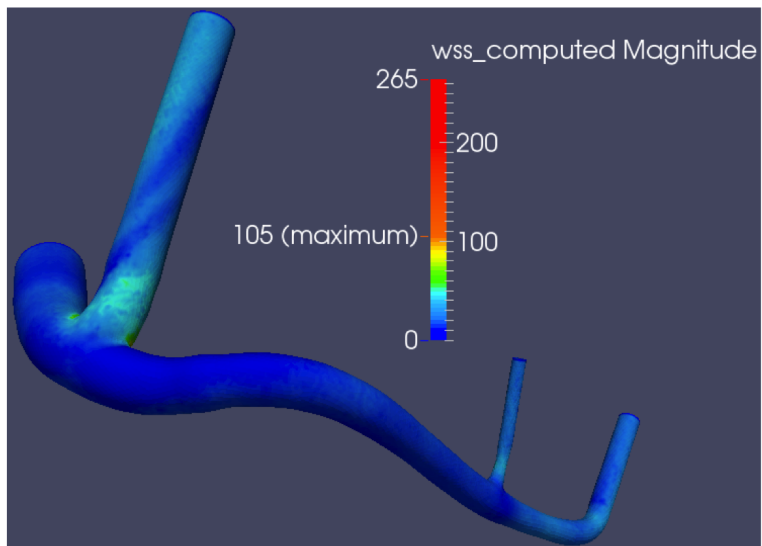
## 5 Conclusion

Comparison of five simulations for different pressures at outflow boundaries and with same velocities at inflow boundaries show that the variations of boundary pressures will generate different blood pressures but have no impact either on the resulting blood velocities and on the related atherosclerosis risk indices, WSS, TAWSS, and OSI. At this point in the study it can be concluded that inaccurate blood pressure measurements in clinic will not affect adversely the prediction of atherosclerosis.

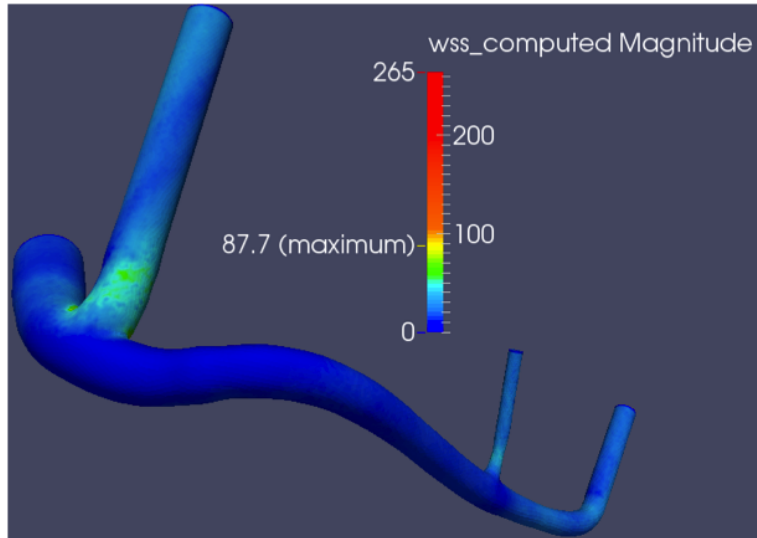
There are two potential paths in which the extensions of this research may proceed. First is to implement the same simulations with a finer mesh. As a fine mesh may generate more accurate results, it will be interesting to investigate if the same conclusions as in this study can be drawn. Second is to vary the way of introducing errors to the outflow boundary



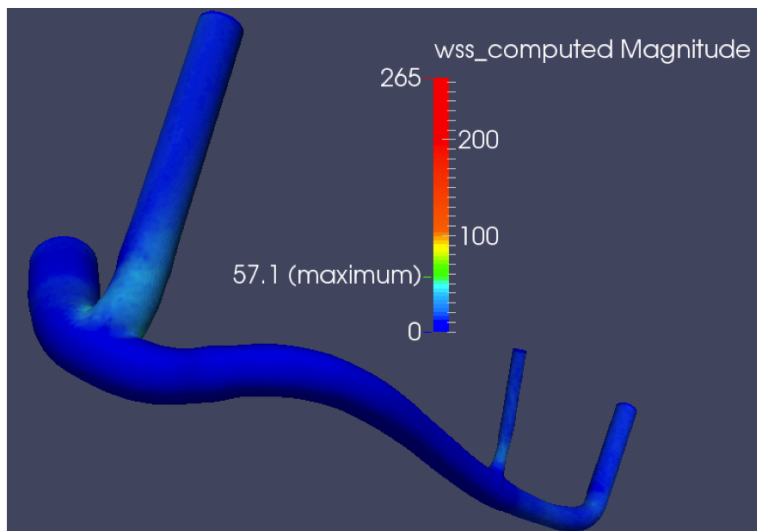
(a) Wall shear stress distribution at time 0.09163s



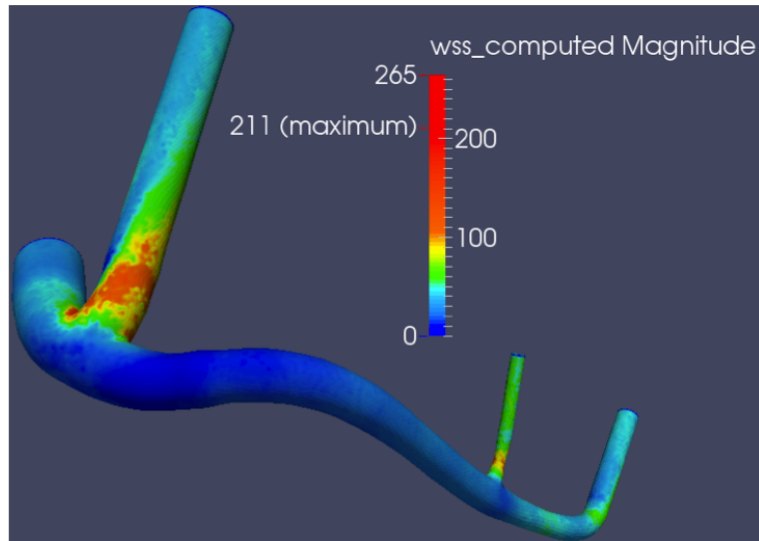
(b) Wall shear stress distribution at time 0.19992s



(c) Wall shear stress distribution at time 0.25823s



(d) Wall shear stress distribution at time 0.3332s



(e) Wall shear stress distribution at time 0.79135s

Figure 13: Evolution of wall shear stress distributions on the vessel wall with the corresponding ranges are visually identical across all the cases at each time point within a complete cardiac cycle

pressures. It will be interesting to investigate how these discrepancies of pressures on the three outflow sections will affect the resulting WSS, OSI and TAWSS.

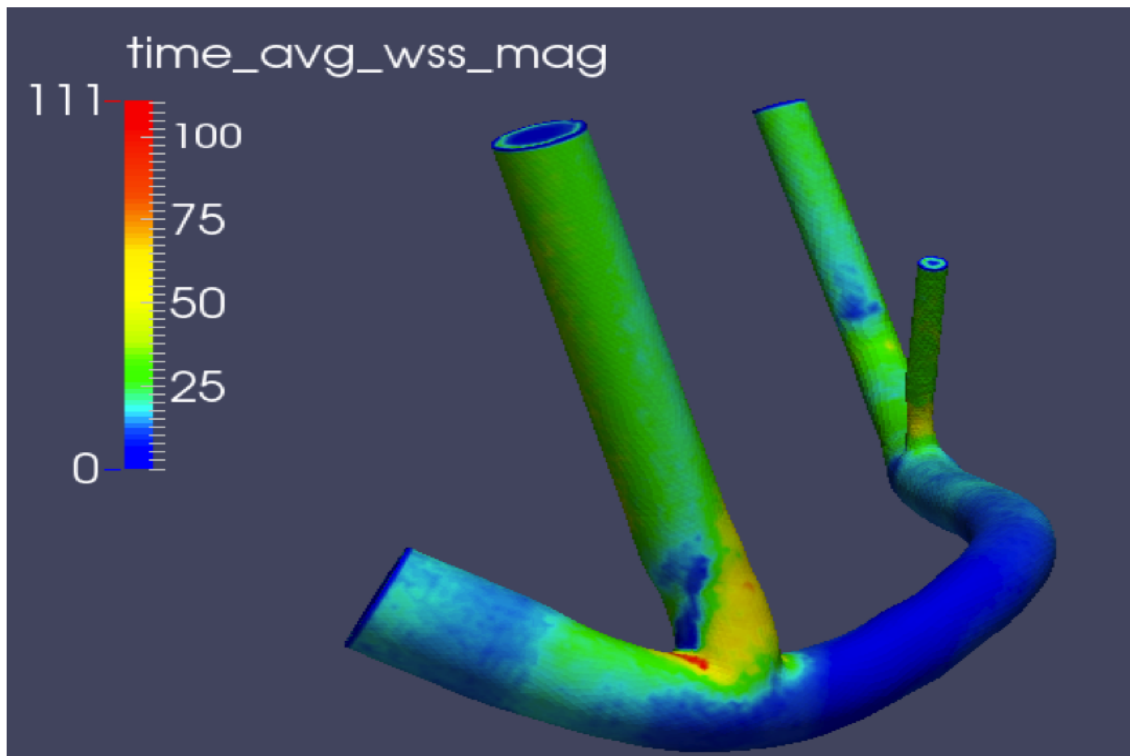


Figure 14: Distributions of time average WSS magnitudes are visually identical in all the cases where pressure is decreased by 20% or by 10%, pressure is patient specific (baseline), pressure is increased by 20% , increased by 10%

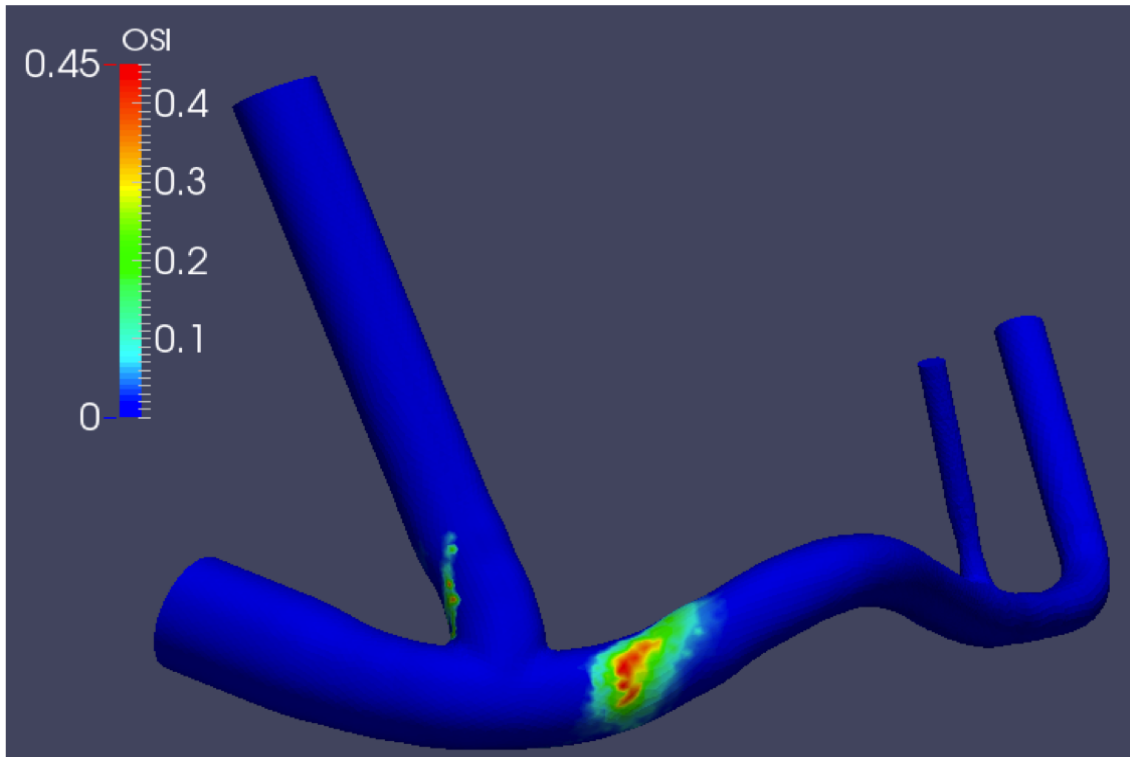
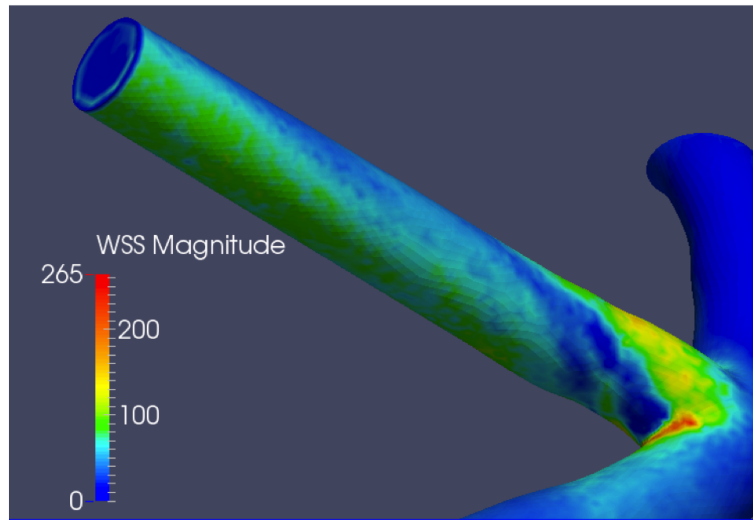
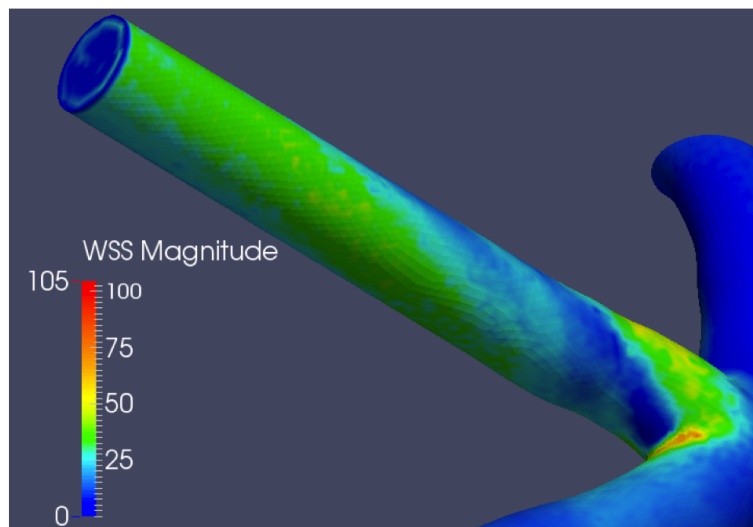


Figure 15: Distributions of OSI magnitudes are visually identical in all the cases where pressure is decreased by 20% or by 10% , original pressure, pressure is increased by 20% , increased by 10%

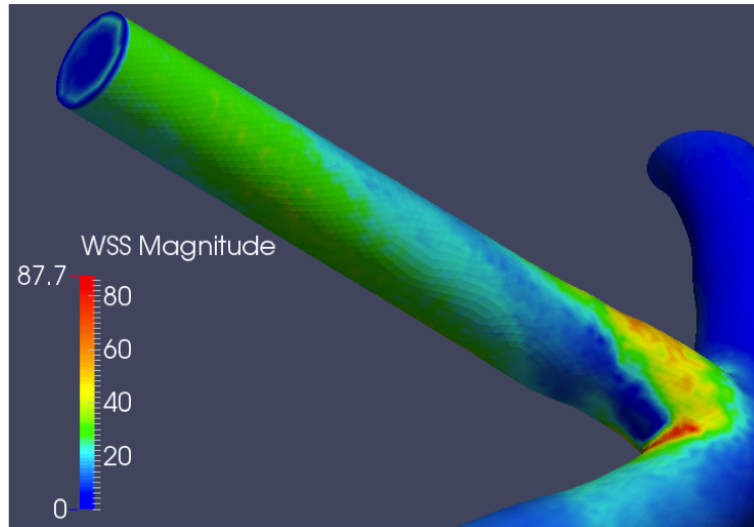




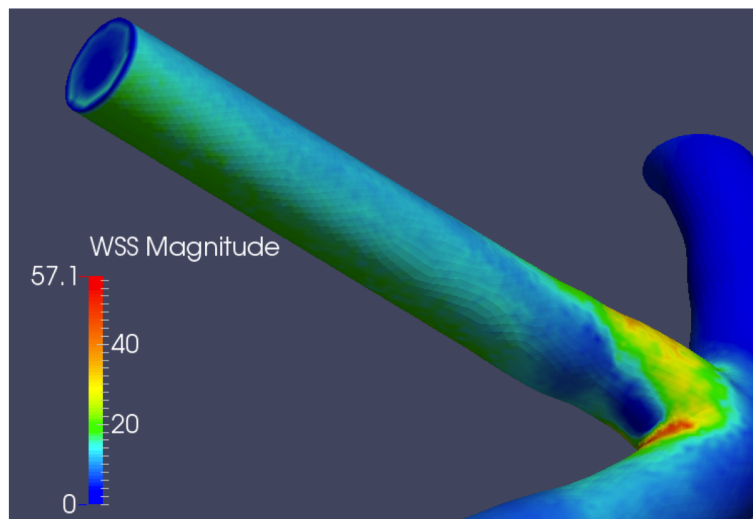
(a) Low wall shear stress distribution at time 0.09163s on the bifurcation area



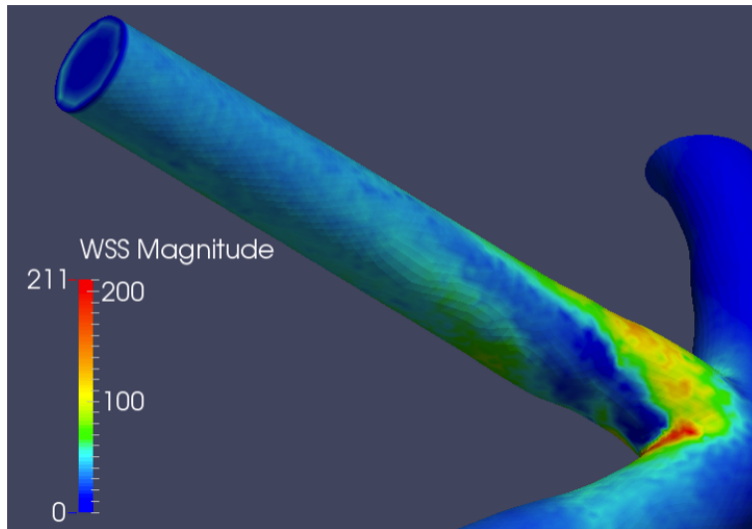
(b) Low wall shear stress distribution on the bifurcation area at time 0.19992s



(c) Low wall shear stress distribution on the bifurcation area at time 0.25823s



(d) Low wall shear stress distribution on the bifurcation area at time 0.3332s

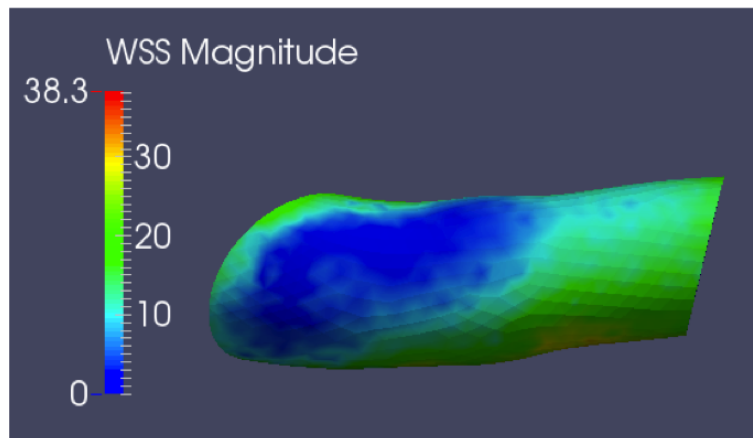


(e) Low wall shear stress distribution on the bifurcation area at time 0.79135s

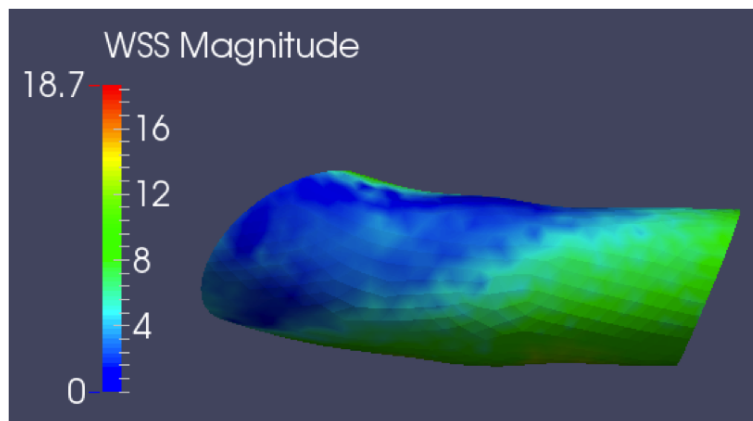
Figure 16: Wall shear stress of the bifurcation area remain low consistently at each time point within a complete cardiac cycle

## 6 Bibliography

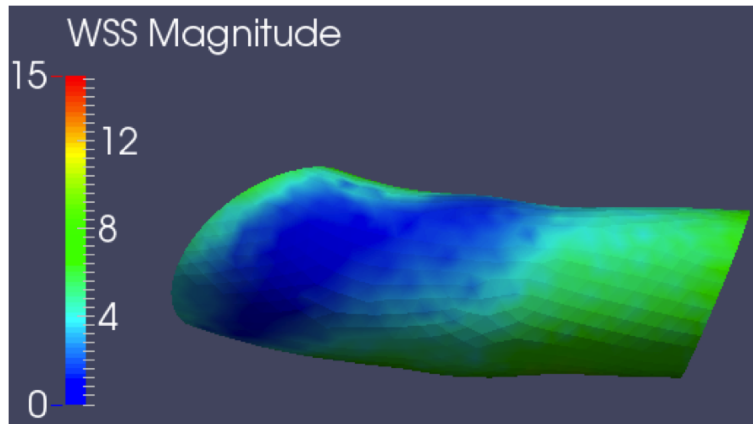
- [1] Coronary artery disease. <http://www.mayoclinic.org/diseases-conditions/coronary-artery-disease/basics/definition/con-20032038>, March 2014.
- [2] Lifev. <https://cmcsforge.epfl.ch/doxygen/lifev/>, March 2014.
- [3] Netgen. <http://www.paraview.org/>, March 2014.
- [4] Paraview. [http://sourceforge.net/apps/mediawiki/netgen-mesher/index.php?title=Main\\_Page](http://sourceforge.net/apps/mediawiki/netgen-mesher/index.php?title=Main_Page), March 2014.
- [5] Oguz K Baskurt, Herbert J Meiselman, et al. Blood rheology and hemodynamics. In *Seminars in thrombosis and hemostasis*, volume 29, pages 435–450. New York: Stratton Intercontinental Medical Book Corporation, c1974, 2003.



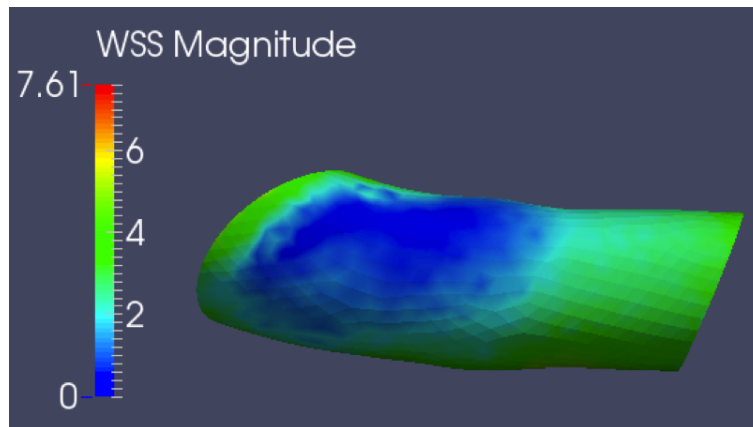
(a) Low wall shear stress distribution at time 0.09163s on part of the main coronary artery



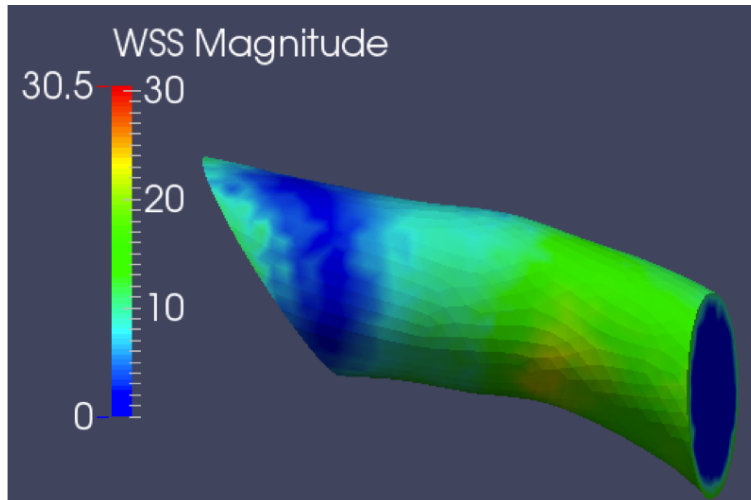
(b) Low wall shear stress distribution on part of the main coronary artery time 0.19992s



(c) Low wall shear stress distribution on part of the main coronary artery at time 0.25823s



(d) Low wall shear stress distribution on part of the main coronary artery at time 0.3332s



(e) Low wall shear stress distribution on part of the main coronary artery at time 0.79135s

Figure 17: Wall shear stress of part of the main coronary artery remain low consistently at each time point within a complete cardiac cycle

- [6] R Baud et al. Numerical investigation of blood flow in the arterial stenosis. *The New Navigators: From Professionals to Patients: Proceedings of MIE2003*, 95:3, 2003.
- [7] Yiannis S Chatzizisis and George D Giannoglou. Coronary hemodynamics and atherosclerotic wall stiffness: a vicious cycle. *Medical hypotheses*, 69(2):349–355, 2007.
- [8] BM Fedorov, TV Sebekina, TM Sinitsyna, EN Strel'tsova, VM Vakulenko, and TG Nikolaeva. [stress and blood circulation in man]. *Kosmicheskaiia biologiiia i aviakosmicheskaiia meditsina*, 24(3):35–40, 1989.
- [9] Luca Formaggia, Alfio M Quarteroni, and Alessandro Veneziani. *Cardiovascular mathematics*. Number CMCS-BOOK-2009-001. Springer, 2009.
- [10] Robert W Gill. Measurement of blood flow by ultrasound: accuracy and sources of error. *Ultrasound in medicine & biology*, 11(4):625–641, 1985.
- [11] S Glagov, Christopher Zarins, DP Giddens, and David N Ku. Hemodynamics and

- atherosclerosis. insights and perspectives gained from studies of human arteries. *Archives of pathology & laboratory medicine*, 112(10):1018–1031, 1988.
- [12] Robin Hart and Elvie Haluszkiewicz. Blood flow velocity using transcranial doppler velocimetry in the middle and anterior cerebral arteries: correlation with sample volume depth. *Ultrasound in medicine & biology*, 26(8):1267–1274, 2000.
- [13] Stanford Hospital and Clinics. Anatomy and function of the coronary arteries. <http://stanfordhospital.org/healthLib/greystone/heartCenter/heartIllustrations/anatomyandFunctionoftheCoronaryArteries.html>, March 2014.
- [14] Yelaswarapu K. *Evaluation of Continuum Models for Characterizing the Constitutive Behavior of Blood*. PhD thesis, University of Pittsburgh, 1996.
- [15] David N Ku. Blood flow in arteries. *Annual Review of Fluid Mechanics*, 29(1):399–434, 1997.
- [16] David N Ku, Don P Giddens, Christopher K Zarins, and Seymour Glagov. Pulsatile flow and atherosclerosis in the human carotid bifurcation. positive correlation between plaque location and low oscillating shear stress. *Arteriosclerosis, Thrombosis, and Vascular Biology*, 5(3):293–302, 1985.
- [17] National Heart Lung and Blood Institute. What is atherosclerosis. <https://www.nhlbi.nih.gov/health/health-topics/topics/atherosclerosis/>, March 2014.
- [18] Adel M Malek, Seth L Alper, and Seigo Izumo. Hemodynamic shear stress and its role in atherosclerosis. *Jama*, 282(21):2035–2042, 1999.
- [19] Alberto Marzo, Pankaj Singh, Ignacio Larrabide, Alessandro Radaelli, Stuart Coley, Matt Gwilliam, Iain D Wilkinson, Patricia Lawford, Philippe Reymond, Umang Patel, et al. Computational hemodynamics in cerebral aneurysms: the effects of modeled versus measured boundary conditions. *Annals of biomedical engineering*, 39(2):884–896, 2011.

- [20] Annalisa Quaini, Tiziano Passerini, Umberto Villa, Alessandro Veneziani, and Suncica Canic. Validation of an open source framework for the simulation of blood flow in rigid and deformable vessels. *MODELLING OF PHYSIOLOGICAL FLOWS*, page 52, 2013.
- [21] Alessandro Veneziani. *Mathematical and numerical modelling of blood flow problems*. PhD thesis, UNIVERSITA DEGLI STUDI DI MILANO POLITECNICO DI MILANO.
- [22] Prem Venugopal, Daniel Valentino, Holger Schmitt, J Pablo Villablanca, Fernando Viñuela, and Gary Duckwiler. Sensitivity of patient-specific numerical simulation of cerebral aneurysm hemodynamics to inflow boundary conditions. *Journal of neurosurgery*, 106(6):1051–1060, 2007.
- [23] Irene E Vignon-Clementel, C Alberto Figueroa, Kenneth E Jansen, and Charles A Taylor. Outflow boundary conditions for three-dimensional finite element modeling of blood flow and pressure in arteries. *Computer methods in applied mechanics and engineering*, 195(29):3776–3796, 2006.
- [24] M Zhao, S Amin-Hanjani, S Ruland, AP Curcio, L Ostergren, and FT Charbel. Regional cerebral blood flow using quantitative mr angiography. *American Journal of Neuroradiology*, 28(8):1470–1473, 2007.